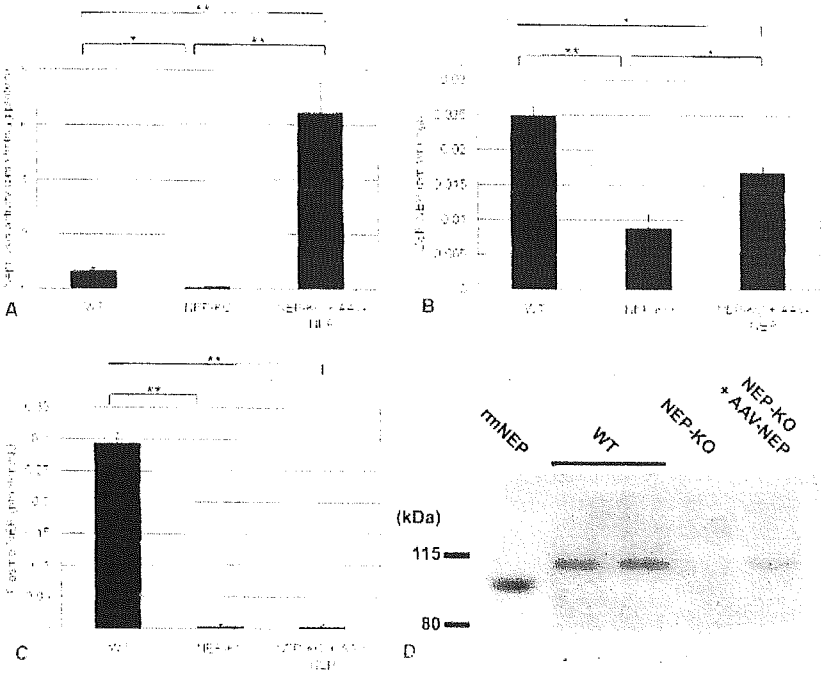

Fig 4. Physiological transfer of neprilysin from the brain into CSF demonstrated by neprilysin-deficient mice injected with recombinant adeno-associated viral vector expressing human neprilysin (rAAV-NEP). (A) Hippocampal neprilysin activity was nearly undetectable in untreated neprilysin-deficient mice (NEP-KO). By contrast, NEP-KO mice at 10 weeks after intrahippocampal rAAV-NEP injection (NEP-KO + AAV-NEP) showed a pronouncedly high level of CSF-NEP, which was approximately 10-fold greater than the endogenous neprilysin activity in wild-type (WT) mice. (B) CSF samples of NEP-KO mice did not produce overt signals compared with those of WT mice. After administration of rAAV-NEP, CSF-NEP in NEP-KO mice was increased to 70% of the endogenous level in WT mice. (C) Unlike CSF-NEP, plasma-NEP did not display an apparent increase after treatment with rAAV-NEP. (D) Immunoblotting of neprilysin in mouse CSF showed consistency with CSF-NEP assay. Each lane was loaded with either CSF sample pooled from three mice or recombinant murine neprilysin (rmNEP). Bars *represent standard error.* $^{*}p < 0.05$; $^{**}p < 0.01$.

untreated neprilysin-deficient mice (see Fig 4C). The transfer of neprilysin from the brains of rAAV-NEP–injected, neprilysin-deficient mice into CSF was also clearly demonstrated by immunoblotting of neprilysin in CSF samples (see Fig 4D). The predominance of the association between neprilysin activities in the brain and CSF over the plasma-CSF correlation suggests strong impacts of brain neprilysin activity on CSF-NEP through transfer of neuronal neprilysin into CSF in physiological conditions.

Pathological Transfer of Neprilysin from the Brain to Cerebrospinal Fluid in Kainic Acid–Treated Rats

In rats injected with KA, there was a KA-induced increase of CSF-NEP in a dose-dependent fashion; low-dose, KA-treated rats showed a slight and insignificant increase of CSF-NEP, and a pronounced increase in CSF-NEP (68-fold greater than the control level) was observed in rats treated with high-dose KA (Fig 5A). Unlike CSF-NEP, plasma-NEP did not significantly differ among the three groups (see Fig 5B). Immunoblotting of neprilysin also indicated a remarkable increase of neprilysin in CSF samples from rats treated with high-dose KA (see Figs 5C [top panel], D [left panel]). In addition to neprilysin, levels of tau in CSF were prominently increased in rats injected with high-dose KA (see Figs 5C [bottom panel], D [right panel]). These data support an aberrantly increased transfer of both neprilysin and tau from damaged brain to CSF, providing a molecular basis for the close association between CSF-NEP and CSF-tau in patients with pMCI and AD (see Figs 2C, D).

Immunoblotting of neprilysin showed that neprilysin in membrane-associated protein fraction from the hippocampi was significantly reduced in rats injected with high-dose KA (Figs 6A, B [left panel]). Neprilysin in Tris/NaCl-soluble fraction had a tendency to increase in KA-treated rats in a dose-dependent fashion, although the increase was not statistically significant (see Figs 6A, B [right panel]). Immunohistochemistry for fragmented α-spectrin indicated extensive activation of calpains in the entire hippocampus except the dentate gyrus after administration of KA at a high dose (see Figs 6C, D). A marked reduction of neprilysin immu-

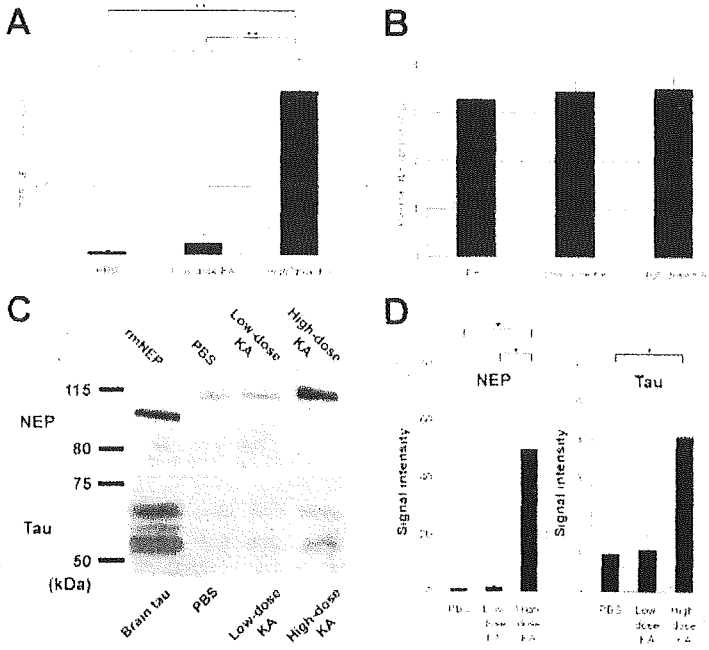

Fig 5. Increased transfer of neprilysin from the brain into cerebrospinal fluid (CSF) in a pathological condition as demonstrated by kainic acid (KA) challenge for rats. (A) Cerebrospinal fluid neprilysin activity (CSF-NEP) was increased after KA administration in a dose-dependent fashion. (B) Plasma-NEP did not significantly differ between rats injected with phosphate-buffered saline and KA. (C) Immunoblotting of neprilysin (top) also indicates a prominent increase of neprilysin in CSF from rats treated with high-dose KA. The CSF sample from a rat injected with high-dose KA was diluted fivefold, and equal volume was loaded in each lane. In addition to neprilysin, levels of tau proteins in CSF (bottom) were significantly increased in rats treated with high-dose KA. Dephosphorylated soluble fraction from rat brain tissue was applied as a control in tau immunoblotting. (D) Intensitometric data constituted from immunoblotting signals demonstrate significant increase in levels of NEP and tau in CSF from rats treated with high-dose KA. Bars *represent standard error.* $^{*}p < 0.05$; $^{**}p < 0.01$.

noreactivity (see Figs 6E, F) accompanying loss of presynaptic signals in interneurons (see Figs 6G, H) was found in the hippocampal CA1 region of the rats treated with high-dose KA compared with the control rats (merged images are shown in Figs 6I, J). These results suggest that increased CSF-NEP in KA-treated rats can be caused by pathological transfer of neprilysin from surface of injured presynaptic membrane to CSF.

Discussion

The principal outcome of this study was to demonstrate that CSF-NEP levels in patients with AD pathologies represent well both down-regulation of brain neprilysin early in the course of the aging-MCI-AD continuum and emanation of neprilysin from damaged neurons with exacerbation of the disease from early to intermediate stages. Importantly, decline of presynaptic neprilysin is putatively one of the earliest cytopathological events in AD pathogenesis[23,24] and is likely to intensify the local concentration of Aβ in the vicinity of synaptic structures. As favored by circumstantial evidence,[25] accumulation of Aβ may disrupt the integrity of synapses, conceivably causing further decrement of presynaptically localized neprilysin. In light of our findings, we conclude that CSF-NEP is potentially an informative biochemical marker to monitor this vicious cycle of synaptic pathogenesis, which can accelerate an imbalance between neprilysin activity and Aβ level in living patients with cognitive deficiency.

A literature of clinical studies has emerged indicating that CSF-tau assay permits prediction of AD-converted MCI and differentiation of prodromal AD from AD-unrelated MCI,[6,7] whereas persistent increase of CSF-tau at a nearly stable level regardless of disease stage[26] may hinder a chance to use CSF-tau as an antemortem index of neuropathological severity of AD. Unlike CSF-tau, CSF-Aβ42 is known to decline as the disease advances[6]; therefore, it may be useful to estimate magnitude of AD pathology in living patients. However, measurement of CSF-Aβ42 does not allow detection of abnormal Aβ metabolism in prodromal AD because of a great overlap among normal, sMCI, and pMCI subjects.[6,27] Based on the data obtained in this study, CSF-NEP assay is capable of distinguishing pMCI patients from normal subjects with a sensitivity of 76% and a specificity of 74% when a cutoff threshold is

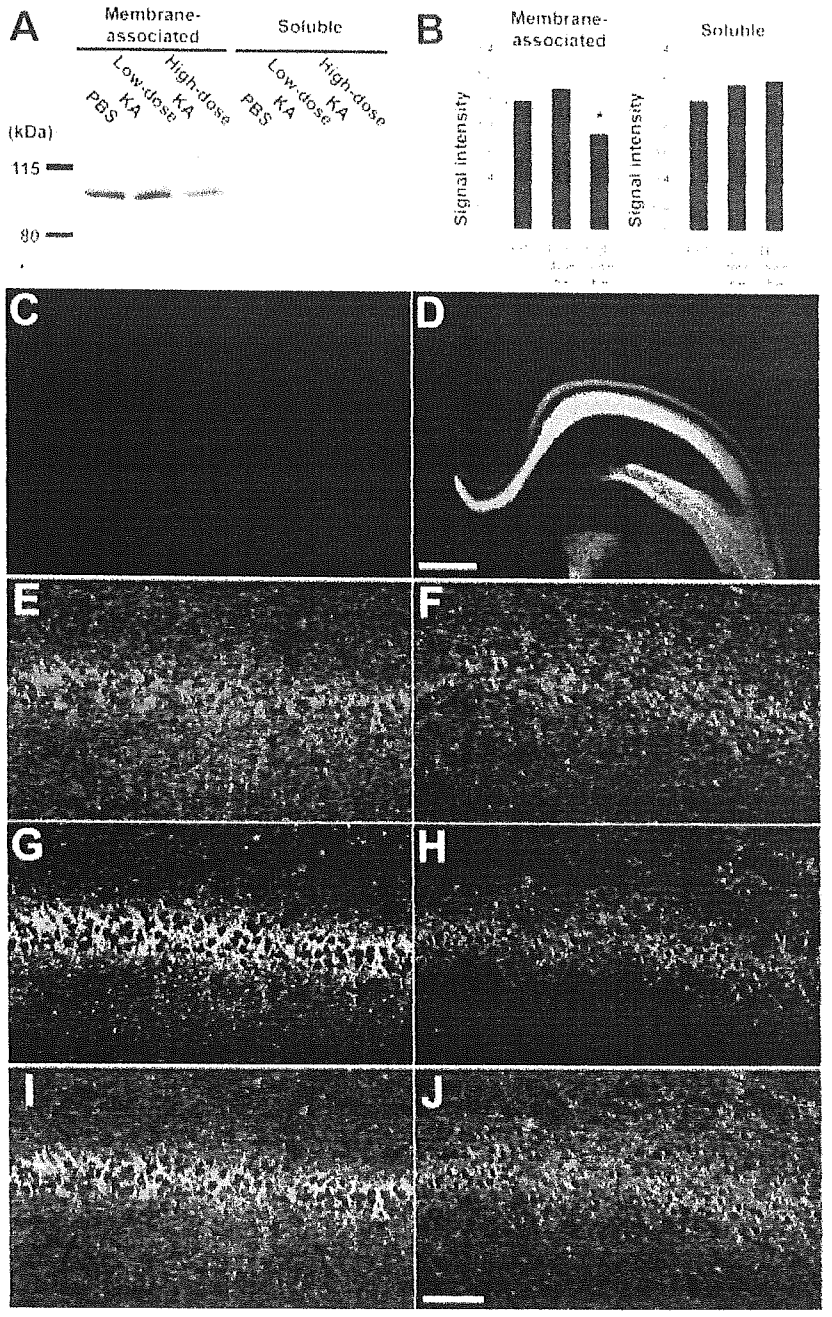

Fig 6. Reduction of neprilysin in disrupted presynaptic terminals observed in the hippocampal formations of rats treated with high-dose kainic acid (KA). (A) Representative immunoblotting indicates reduced level of membrane-associated neprilysin in high-dose KA group. Note that soluble neprilysin exhibits a larger molecular mass than membrane-associated neprilysin, presumably because of a higher magnitude of glycosylation. (B) Significant decrease of membrane-associated neprilysin in rats treated with high-dose KA was demonstrated by intensitometry of neprilysin immunoblotting signals. Bars *represent standard error. (C–J) Immunostaining of hippocampal sections from rats treated with phosphate-buffered saline (left) and high-dose KA (right). Scale bars = 250μm (C, D); 100μm (E–J).* $^{*}p < 0.05$.

assigned at 0.012 pmol/min/μl. These values may not appear particularly impressive as compared with CSF-tau, but they clearly support feasibility of using CSF-NEP as a valuable clinical adjunct to prediction of conversion from MCI to AD in view of Aβ pathogenesis. Moreover, alteration of CSF-NEP as a function of dis-

ease severity enables evaluation of neuropathological progression as patients are longitudinally examined.

It should be noted that a reduction of CSF-NEP in pMCI is indicative of a decreased level of neuronal neprilysin and a consequent diminishment of physiological transfer of neprilysin from the brain to CSF. An increased level of CSF-NEP in neprilysin-deficient mice after intrahippocampal administration of rAAV-NEP has provided unequivocal evidence for such a transfer in nonpathological conditions. The molecular mechanisms by which neprilysin is released from healthy neurons to extracellular matrix remain to be elucidated. Our immunoblotting data indicate release of neprilysin from neurons without enzymatic shedding, unlike other membrane-bound metalloproteases.[28,29] Further biochemical assessments including mass spectrometric analysis of immunocaptured samples are required to identify membrane-unbound species of neprilysin that are transferable to CSF.

As mentioned earlier, the significant association of CSF-NEP with both MMSE score and CSF-tau suggests aberrant release of neprilysin from degenerating neurons. Because there was a lack of a significant correlation between CSF-tau and MMSE score in accordance with previous findings,[26] we postulate that diffusion of neprilysin from the central nervous system to CSF in neurodegeneration has primarily two distinct origins: neurons in the middle of active neuritic and synaptic disruptions, and neurons at the end stage of the degenerative process. Based on a marked and transient increase in CSF-tau levels after acute brain injuries,[30,31] CSF-tau levels supposedly reflect the number of neurons undergoing active degenerative processes. Diffusion of neprilysin from neurons to extracellular medium can first unfold on this acute and active neuropathology, as this experiment demonstrates using KA-treated rats. Neurons at the terminal stage of degenerative changes are unlikely to release a substantial quantity of tau, because tau in such neurons is depleted in the axonal compartment or is stuck to fibrillary aggregates in the somatodendritic compartment, or both.[32] However, advanced stages of cellular injury are presumed to still allow neurons to remain productive of neprilysin, and disruption or instability of membrane structures may promote emanation of neprilysin from these cells. The number of these terminally damaged neurons increases as the disease progresses, leading to an increase of CSF-NEP in tight association with disease severity.

Our data also suggest potential benefits of neprilysin up-regulation in treating patients with pMCI and mild AD and usefulness of CSF-NEP for biochemically evaluating efficacy of the treatment in these patients. In fact, suppression of Aβ levels and amyloid plaque formation in amyloid precursor protein transgenic mice by genetically up-regulating neprilysin has been demonstrated by several independent groups.[11,33,34] Possibility of pharmacological modulation of regulatory mechanisms for neprilysin activity has also been raised by various lines of supportive evidence.[23,35] CSF-NEP could have a predictive value for identifying who would be a responder to neprilysin activation among patients with pMCI and early-stage AD.

In conclusion, this study has provided strong clinical and experimental indication that compromised neprilysin activity, Aβ-triggered neuronal injury, and a conjunction of these two changes in the brain can be monitored by CSF-NEP assay from predementia phase of AD. Quantification of CSF-NEP may also play a role in the diagnostic work-up of MCI to identify patients in transition from MCI to AD and patients afflicted by a depletion of brain neprilysin. This will be of particular importance when drugs with potential up-regulatory effects on neprilysin activity reach the clinical trial stage.

This work was supported by a grant from RIKEN BSI (M.H., Y.J., N.I.; T.S.).

We thank Dr C. Gerard at Harvard Medical School for providing neprilysin-deficient mice and M. Sekiguchi for technical assistance. We appreciate the patients and their families who made our research possible through their generous efforts to foster research.

References

1. Saido TC. Aβ metabolism: from Alzheimer research to brain aging control. In: Saido TC, ed. Aβ metabolism and Alzheimer's disease. Georgetown, TX: Landes Bioscience, 2003:1–16.
2. Hardy J, Selkoe DJ. The amyloid hypothesis of Alzheimer's disease: progress and problems on the road to therapeutics. Science 2002;297:353–356.
3. Motter R, Vigo-Pelfrey C, Kholodenko D, et al. Reduction of beta-amyloid peptide (42) in the cerebrospinal fluid of patients with Alzheimer's disease. Ann Neurol 1995;38:643–648.
4. Arai H, Terajima M, Miura M, et al. Tau in cerebrospinal fluid: a potential diagnostic marker in Alzheimer's disease. Ann Neurol 1995;38:649–652.
5. Growdon JH. Biomarkers of Alzheimer disease. Arch Neurol 1999;56:281–283.
6. Maruyama M, Arai H, Sugita M, et al. Cerebrospinal fluid amyloid beta(1-42) levels in the mild cognitive impairment stage of Alzheimer's disease. Exp Neurol 2001;172:433–436.
7. Okamura N, Arai H, Maruyama M, et al. Combined analysis of CSF tau levels and [^{123}I]iodoamphetamine SPECT in mild cognitive impairment: implications for a novel predictor of Alzheimer's disease. Am J Psychiatry 2002;159:474–476.
8. Doody RS. Current treatments for Alzheimer's disease: cholinesterase inhibitors. J Clin Psychiatry 2003;64(suppl 9):11–17.
9. Dodel RC, Hampel H, Du Y. Immunotherapy for Alzheimer's disease. Lancet Neurol 2003;2:215–220.
10. Scarpini L, Scheltens P, Feldman H. Treatment of Alzheimer's disease: current status and new perspectives. Lancet Neurol 2003;2:539–547.
11. Iwata N, Tsubuki S, Takaki Y, et al. Identification of the major $A\beta_{1-42}$-degrading catabolic pathway in brain parenchyma: suppression leads to biochemical and pathological deposition. Nat Med 2000;6:143–150.
12. Iwata N, Tsubuki S, Takaki Y, et al. Metabolic regulation of brain Aβ by neprilysin. Science 2001;292:1550–1552.

13. Fukami S, Watanabe K, Iwata N, et al. Aβ-degrading endopeptidase, neprilysin, in mouse brain: synaptic and axonal localization inversely correlating with Aβ pathology. Neurosci Res 2002;43:39–56.
14. Iwata N, Mizukami H, Shirotani K, et al. Presynaptic localization of neprilysin contributes to efficient clearance of amyloid-beta peptide in mouse brain. J Neurosci 2004;24:991–998.
15. Yasojima K, Akiyama H, McGeer EG, McGeer PL. Reduced neprilysin in high plaque areas of Alzheimer brain: a possible relationship to deficient degradation of beta-amyloid peptide. Neurosci Lett 2001;297:97–100.
16. Maruyama M, Matsui T, Tanji H, et al. Cerebrospinal fluid tau protein and periventricular white matter lesions in patients with mild cognitive impairment: implications for 2 major pathways. Arch Neurol 2004;61:716–720.
17. Petersen RC, Doody R, Kurz A, et al. Current concepts in mild cognitive impairment. Arch Neurol 2001;58:1985–1992.
18. McKhann G, Drachman D, Folstein M, et al. Clinical diagnosis of Alzheimer's disease: report of the NINCDS-ADRDA Work Group under the auspices of Department of Health and Human Services Task Force on Alzheimer's Disease. Neurology 1984;34:939–944.
19. Hama E, Shirotani K, Iwata N, Saido TC. Effects of neprilysin chimeric proteins targeted to subcellular compartments on amyloid beta peptide clearance in primary neurons. J Biol Chem 2004;279:30259–30264.
20. Edge AS. Deglycosylation of glycoproteins with trifluoromethanesulphonic acid: elucidation of molecular structure and function. Biochem J 2003;376:339–350.
21. DeMattos RB, Bales KR, Parsadanian M, et al. Plaque-associated disruption of CSF and plasma amyloid-β (Aβ) equilibrium in a mouse model of Alzheimer's disease. J Neurochem 2002;81:229–236.
22. Saido TC, Yokota M, Nagao S, et al. Spatial resolution of fodrin proteolysis in postischemic brain. J Biol Chem 1993;268:25239–25243.
23. Saito T, Takaki Y, Iwata N, et al. Alzheimer's disease, neuropeptides, neuropeptidase, and amyloid-beta peptide metabolism. Sci Aging Knowledge Environ 2003;2003:PE1.
24. Saido TC, Nakahara H. Proteolytic degradation of Aβ by neprilysin and other peptidases. In: Saido TC, ed. Aβ metabolism and Alzheimer's disease. Georgetown, TX: Landes Bioscience, 2003:61–80.
25. Selkoe DJ. Alzheimer's disease is a synaptic failure. Science 2002;298:789–791.
26. Itoh N, Arai H, Urakami K, et al. Large-scale, multicenter study of cerebrospinal fluid tau protein phosphorylated at serine 199 for the antemortem diagnosis of Alzheimer's disease. Ann Neurol 2001;50:150–156.
27. Jensen M, Schroder J, Blomberg M, et al. Cerebrospinal fluid A β42 is increased early in sporadic Alzheimer's disease and declines with disease progression. Ann Neurol 1999;45:504–511.
28. Chubinskaya S, Mikhail R, Deutsch A, Tindal MH. ADAM-10 protein is present in human articular cartilage primarily in the membrane-bound form and is upregulated in osteoarthritis and in response to IL-1alpha in bovine nasal cartilage. J Histochem Cytochem 2001;49:1165–1176.
29. Osenkowski P, Toth M, Fridman R. Processing, shedding, and endocytosis of membrane type 1-matrix metalloproteinase (MT1-MMP). J Cell Physiol 2004;200:2–10.
30. Hesse C, Rosengren L, Vanmechelen E, et al. Cerebrospinal fluid markers for Alzheimer's disease evaluated after acute ischemic stroke. J Alzheimers Dis 2000;2:199–206.
31. Franz G, Beer R, Kampfl A, et al. Amyloid beta 1-42 and tau in cerebrospinal fluid after severe traumatic brain injury. Neurology 2003;60:1457–1461.
32. Higuchi M, Lee VM, Trojanowski JQ. Tau and axonopathy in neurodegenerative disorders. Neuromolecular Med 2002;2:131–150.
33. Marr RA, Rockenstein E, Mukherjee A, et al. Neprilysin gene transfer reduces human amyloid pathology in transgenic mice. J Neurosci 2003;23:1992–1996.
34. Leissring MA, Farris W, Chang AY, et al. Enhanced proteolysis of beta-amyloid in APP transgenic mice prevents plaque formation, secondary pathology, and premature death. Neuron 2003;40:1087–1093.
35. Saito T, Iwata N, Tsubuki S, et al. Somatostatin regulates brain amyloid β peptide, $A\beta_{42}$, through modulation of proteolytic degradation. Nat Med 2005;11:434–439.

doi:10.1016/j.ymthe.2005.03.021

ARTICLE

Specific and Efficient Transduction of *Cochlear* Inner Hair Cells with Recombinant Adeno-associated Virus Type 3 Vector

Yuhe Liu,[1,2] Takashi Okada,[1] Kianoush Sheykholeslami,[3] Kuniko Shimazaki,[4] Tatsuya Nomoto,[1] Shin-Ichi Muramatsu,[5] Takeharu Kanazawa,[6] Koichi Takeuchi,[7] Rahim Ajalli,[2] Hiroaki Mizukami,[1] Akihiro Kume,[1] Keiichi Ichimura,[2] and Keiya Ozawa[1,*]

[1]*Division of Genetic Therapeutics, Center for Molecular Medicine, Jichi Medical School, 3311-1 Yakushiji, Minami-kawachi, Kawachi, Tochigi 329-0498, Japan*
[2]*Department of Otolaryngology and Head and Neck Surgery, Jichi Medical School, 3311-1 Yakushiji, Minami-kawachi, Kawachi, Tochigi 329-0498, Japan*
[3]*Department of Neurobiology, Northeastern Ohio Universities College of Medicine, Rootstown, OH 44272, USA*
[4]*Department of Physiology, Jichi Medical School, 3311-1 Yakushiji, Minami-kawachi, Kawachi, Tochigi 329-0498, Japan*
[5]*Department of Medicine, Division of Neurology, Jichi Medical School, 3311-1 Yakushiji, Minami-kawachi, Kawachi, Tochigi 329-0498, Japan*
[6]*Department of Otolaryngology and Head and Neck Surgery, Faculty of Medicine, University of the Ryukyus, Okinawa 903-0213, Japan*
[7]*Department of Anatomy, Jichi Medical School, 3311-1 Yakushiji, Minami-kawachi, Kawachi, Tochigi 329-0498, Japan*

**To whom correspondence and reprint requests should be addressed. Fax: (+81) 285 44 8675. E-mail: kozawa@jichi.ac.jp.*

Available online 12 May 2005

Recombinant adeno-associated virus (AAV) vectors are of interest for cochlear gene therapy because of their ability to mediate the efficient transfer and long-term stable expression of therapeutic genes in a wide variety of postmitotic tissues with minimal vector-related cytotoxicity. In the present study, seven AAV serotypes (AAV1–5, 7, 8) were used to construct vectors. The expression of EGFP by the chicken β-actin promoter associated with the cytomegalovirus immediate-early enhancer in cochlear cells showed that each of these serotypes successfully targets distinct cochlear cell types. In contrast to the other serotypes, the AAV3 vector specifically transduced cochlear inner hair cells with high efficiency *in vivo*, while the AAV1, 2, 5, 7, and 8 vectors also transduced these and other cell types, including spiral ganglion and spiral ligament cells. There was no loss of cochlear function with respect to evoked auditory brain-stem responses over the range of frequencies tested after the injection of AAV vectors. These findings are of value for further molecular studies of cochlear inner hair cells and for gene replacement strategies to correct recessive genetic hearing loss due to monogenic mutations in these cells.

Key Words: adeno-associated virus, serotype, gene transfer, cochlea, hair cells

INTRODUCTION

The total number of hair cells in the cochlea is finite. They are not renewed and there is very little (if any) redundancy in this population. The irreversible loss of cochlear hair cells is presumed to be a fundamental cause of permanent sensorineural hearing loss. Gene transfer into hair cells presents numerous opportunities for protecting these cells. There is considerable interest in the development of viral vectors to deliver genes to the cochlea to counteract hearing impairment, and recent studies have focused on vectors based on adenovirus [1–3], herpes simplex virus [4–6], lentivirus [7], and adeno-associated virus (AAV) [8,9]. The patterns of vector-encoded transgene expression have been found to differ significantly among vectors. Cochlear hair cells can be efficiently transduced with adenovirus vectors [10–12]. However, these vectors were found to provoke a strong immune response that could damage recipient cells and compromise cochlear function [10,13,14]; they are also incapable of mediating prolonged transgene expression [15,16]. Although AAV vectors might overcome these problems, the transduction of hair cells by AAV2-derived vectors is controversial [8,10,17]. To our knowledge, other AAV serotypes have not yet been tested as cochlear gene transfer vectors *in vitro* or *in vivo*. AAV vectors are of interest in the context of gene therapy because they mediate efficient transfer and long-term stable expression of therapeutic genes in a wide variety of postmitotic tissues with minimal vector-related cytotoxicity.

In this study, we assessed the utility of seven AAV serotypes as vectors with the chicken β-actin promoter associated with a cytomegalovirus immediate-early

1525-0016/$30.00

doi:10.1016/j.ymthe.2005.03.021

enhancer (CAG)-driven enhanced green fluorescent protein (EGFP) gene [18] in the murine cochlea. Vectors were introduced by microinjection through the round window membrane [19]. As a result, we determined that the specific and efficient gene transduction of inner hair cells could be achieved by using AAV type 3 vectors.

RESULTS

Expression Profile of EGFP in the Cochlea

Several cell types line the cochlear duct and support the hair cells (Fig. 1A). We carefully made a small opening in the tympanic bulla and injected vectors derived from the AAV1–4, 7, and 8 pseudotypes into the cochlea of two strains of mice (C57BL/6J and ICR) through the round window membrane (Fig. 1B). The mode of EGFP expression in various murine cochlear hair cells had a close similarity and was essentially equal for both strains. We determined the distribution of AAV vector-mediated EGFP expression throughout the cochlea for all serotypes tested (Table 1). A principal finding is that the inner hair cells in the organ of Corti showed clear evidence of EGFP expression with all of the AAV serotype-derived vectors except for the AAV4 vector (Fig. 2). This result indicates that most of the vectors (AAV1–5, 7, and 8) could efficiently transduce cochlear inner hair cells *in vivo* when slowly infused into the scala tympani. The AAV3-based vector was the most efficient and specific of the serotypes in transducing cochlear inner hair cells (Fig. 3). Transduction with 5×10^{10} genome copies (gc)/cochlea of the AAV3 vector resulted in robust transgene expression in the inner hair cells. The spiral ganglion cells showed significantly higher levels of fluorescence per unit area with the AAV5-based vector (Fig. 2n), and the spiral ligament cells were transduced prominently with the AAV1 and AAV7 vectors (Figs. 2d and 2r). Histological sections of cochleae injected with the AAV4 vector identified EGFP-positive cells predominantly in connective tissue within the mesothelial cells beneath the organ of Corti and in mesenchymal cells lining the perilymphatic fluid spaces (Figs. 2j and 2l). Furthermore, we detected intense expression with the AAV5- and AAV8-based vectors in the inner sulcus cells and in Claudius' cells (Figs. 2p and 2x). We did not detect notable levels of gene expression in the outer hair cells, supporting pillar cells, or stria vascularis cells for any serotype.

Long-term Expression of EGFP

We examined cochlear expression of the EGFP transgene in animals sacrificed at 1–12 weeks. Expression persisted in cochlear tissues for up to 3 months after infusion, while the extent of expression peaked at 2 weeks.

Transgene Activity

We determined the percentage of inner hair cells transduced with the AAV3 vector. The mid- to high-frequency regions of the cochlea were efficiently transduced, as shown in Fig. 3. Almost all of the inner hair cells in the basal and middle cochlear regions were transduced with the AAV3 vector (Fig. 4). Transgene expression was not detected in the hair cells of the apical turn of the cochlea. The predominant expression in the middle and basal cochlear turns is reasonable, as the virus

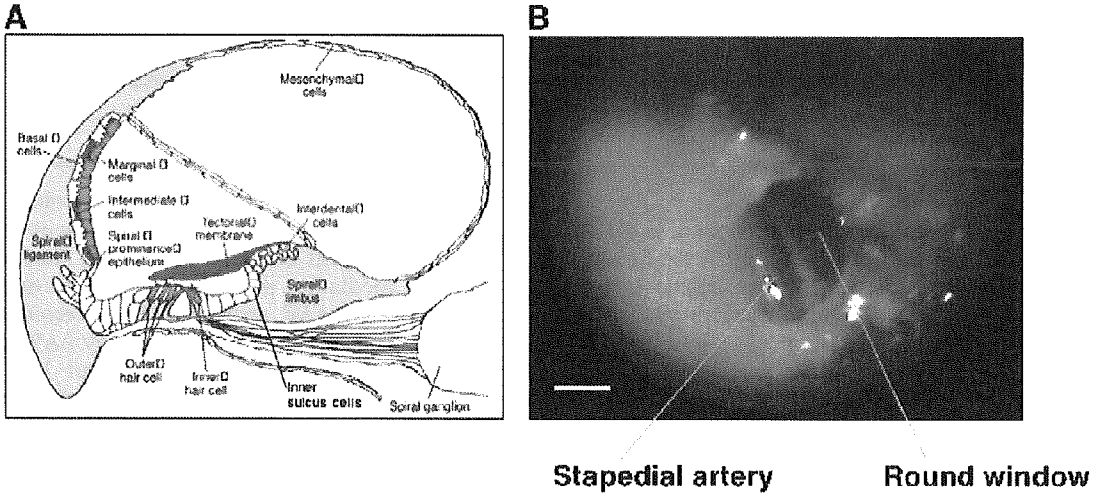

FIG. 1. (A) Schematic diagram of a cross section of the cochlea, demonstrating the scala vestibuli, scala tympani, and scala media or cochlear duct. The organ of Corti rests on the basilar membrane, with the hair cell cilia embedded in the gelatinous tectorial membrane. The outer margin of the cochlear duct contains the stria vascularis. Reproduced, by permission of the publisher, from [44]. (B) Direct visualization of the round window membrane in the right ear. The upper side of the picture is the back of the mouse and the right side is the head of the animal. The stapedial artery, a branch of the internal carotid artery, transverses an open bony semicanal within the round window niche. Bar denotes 500 μm, 15× original magnification.

TABLE 1: Expression of transgene in the mouse cochlea with vectors derived from the AAV1–4, 7, and 8 pseudotypes

Vector	Inner hair cells	Outer hair cells	Spiral ganglion	Stria vascularis	Spiral ligament	Spiral limbus	Reissner's membrane	Inner and outer pillar cells	Inner sulcus cells	Deiter's cells	Claudius' cells	Hensen's cells	Mesenchymal cells
AAV1	+++	–	++	–	++	++	++	–	+	–	–	–	++
AAV2	++	–	+	–	+	+	–	–	–	–	–	–	–
AAV3	++++	–	–	–	–	–	–	–	–	–	–	–	–
AAV4	–	–	–	–	–	–	–	–	–	–	–	–	+
AAV5	+++	–	+++	–	+	++	+	–	++	–	+	–	–
AAV7	+++	–	+	–	+++	++	–	–	+	–	+	–	++
AAV8	++++	–	–	–	+	+	–	–	++	–	+	–	+

The level of expression was graded by fluorescence intensity on a four-level scale (+, ++, +++, ++++) depending on the pixel/unit area count. ++++ means the strongest intensity of EGFP expression, + means the weakest intensity of EGFP expression, while – means no fluorescence.

was slowly infused into the scala tympani adjacent to the most basal turn of the cochlea. The percentage of transduced inner hair cells from the basal (high frequencies) to the apical (low frequencies) cochlear regions is shown in Fig. 4.

Cytotoxicity

We detected no deleterious effects on the viability of transduced cells. We compared evoked auditory brainstem response (ABR) threshold levels before and after injection, using a two-way repeated measure of the analysis of variance. There was no significant loss in ABR and hence no change in cochlear function for up to 10 days following vector infusion (Figs. 5A and 5B). In addition, the cellular and tissue architecture of experimental cochleae remained intact. There was no evidence of endolymphatic hydrops after AAV vector injection in any of the animals. We observed no significant destruction of the inner or outer hair cells (Fig. 5C).

Discussion

In the present study, we assessed the utility of vectors derived from seven AAV serotypes for gene delivery into the cochlea. Our results showed that the AAV3 vector was the most efficient and specific in transducing cochlear inner hair cells, although these cells could also be transduced with AAV1, 2, 5, 7, and 8 vectors. The transduction efficiency of the spiral ganglion by the AAV5 vector was particularly high, followed by that of the AAV1, AAV2, and AAV7 vectors. The efficient and specific transduction of inner hair cells with the AAV3 vector suggests that it recognizes a unique host range with a distinct cellular receptor. Transduction efficiency is dependent on initial viral binding (a property of the viral capsid), entry, and various postentry processes such as intracellular trafficking and second-strand synthesis [20–22]. The genome size of AAV vectors has also been demonstrated to affect transduction efficiency [23]. Comparisons of the serotypes have indicated that heterogeneity in the capsid-encoding regions and a differential ability to transduce cells may be associated with different receptor and co-receptor requirements for cell entry [24]. However, the receptors and co-receptors of AAV3 have not yet been clearly identified.

In the current study, we found that cochlear inner hair cells could be transduced with six AAV serotypes, although Lalwini *et al.* [8] reported that outer hair cells could be transduced with a low titer (1×10^6 viral particles/ml) of AAV2 *in vivo*. After injecting the AAV2 vector, we found that the spiral ganglion neurons, the inner hair cells, and the cells in the spiral ligament were all transduced. This transduction pattern differs from that reported in previous studies [8,10,17], and this discrepancy might be due to the different delivery methods and dissimilar promoters. Although the CAG promoter directs

doi:10.1016/j.ymthe.2005.03.021

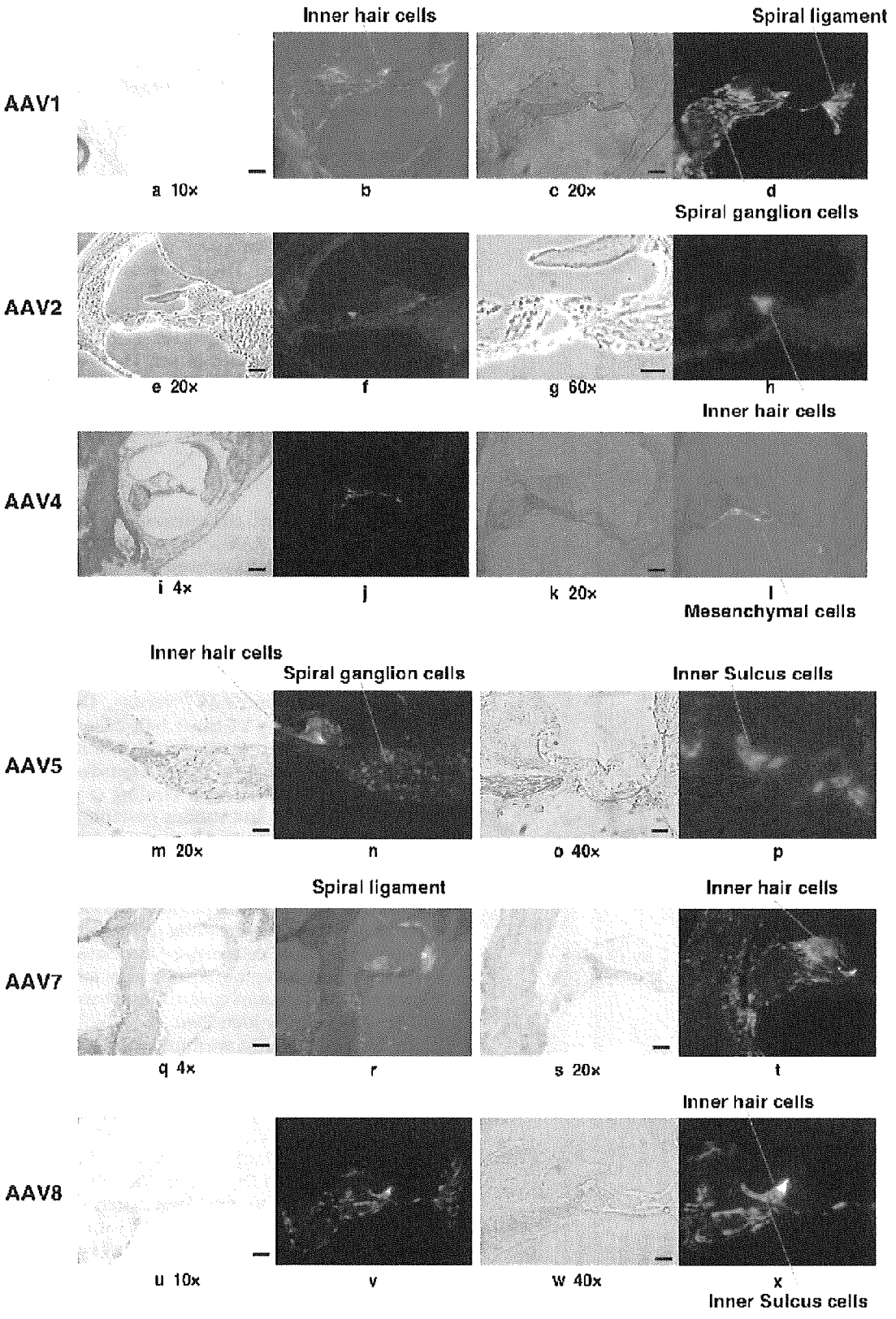

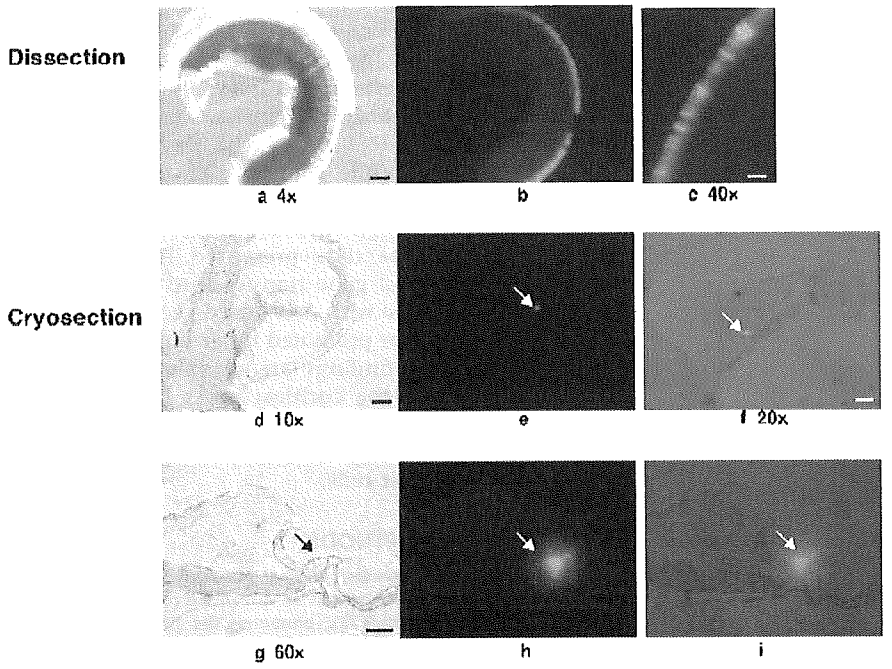

FIG. 3. Cochlear transduction with AAV3-CAG-EGFP. Dissected cochleae and cryosections show transgene expression in inner hair cells. (a) A light photomicrograph of the basal turn of the cochlea is shown, illustrating its laminar structure. (b) A fluorescence photomicrograph of this dissection. (c) A higher magnification view of the dissection shown in (b), illustrating a row of inner hair cells in the organ of Corti expressing EGFP. (d–i) Representative photomicrographs from three magnifications of a radial cochlear cryosection. (d) Light photomicrography of an intact cochlear duct. Fluorescence photomicrography of this duct is shown in (e). (h and i) A higher magnification of (e), illustrating EGFP expression within inner hair cells. Cryosections show transgene expression in the inner hair cells (arrows). Scale bars: 4×, 250 μm; 10×, 100 μm; 20×, 50 μm; 40×, 25 μm; 60×, 25 μm.

higher expression than do the cytomegalovirus (CMV) and EF-1α promoters [25], each promoter drives reporter gene expression in different cell types [26,27].

Cell-specific or -selective infectivity of the viral vectors suggests the presence of various factors to introduce the distinct expression patterns of the transgenes. Spiral ganglion neurons and glial cells can be transduced with a lentivirus–GFP construct *in vitro* but not *in vivo* [7]. The differential transducibility under *in vivo* and *in vitro* conditions reflects a high degree of structural isolation of the spiral ganglion and other cell types—such as the cells on the periphery of the endolymph—from the perilymph into which the viral vector was introduced. The strict separation of the endolymph from the perilymph is maintained by tight junctions that line the boundary between these fluid chambers. The size of the viral particle may contribute to the observed variability in transgene expression promoted by different vectors. The diameters of adenovirus and retrovirus (including lentivirus) particles are approximately 75 nm and greater than 100 nm, respectively, while the diameters of AAV vectors are typically 11–22 nm [28,29]. Thus, the larger size of lentiviruses and adenoviruses may limit their subsequent dissemination from the perilymph into the endolymph. The variable patterns of adenovirus- and lentivirus-mediated gene expression seen with different methods of inoculation may be due to the inoculation route, the volume and number of viral particles, differences in viral preparation, or differences in the method of transgene detection. The introduction of adenovirus vectors by cochleostomy or with an osmotic pump via the round window leads to a more efficient transduction of cochlear hair cells [30–32]. The apical domain (apical membrane and stereocilia) of cells in the sensory epithelium (hair cells and supporting cells) is bathed in endolymph, while the basal–lateral domain is immersed in perilymph. Access of the viral vectors to the endolymphatic space by cochleostomy may facilitate the transduction of hair cells and supporting cells. However, although the cochleostomy procedure has been tested, inoculation into the membranous labyrinth could not be confirmed [32]. In the present study, AAV vectors were found to infect cochlear hair cells easily *in vivo,* via round window injection.

Gene transfer into the cochlea through the round window membrane is ideal, because this procedure

FIG. 2. Transduction of the cochleae by AAV1-, AAV2-, AAV4-, AAV5-, AAV7-, and AAV8-based vectors. (a, c, e, g, i, k, m, o, q, s, u, and w) Light photomicrographs of cochlear cryosections. (b, d, f, h, j, l, n, p, r, t, v, and x) Fluorescence photomicrographs (green fluorescence from transgene). The spiral ligament cells were transduced prominently with the AAV1 and AAV7 vectors (d and r). Transgene expression in inner hair cells was detected with AAV1-, AAV2-, AAV5-, AAV7-, and AAV8-based vectors (b, h, n, t, and x). AAV4-based vector faintly transduced mesenchymal cells (j and l). The spiral ganglion cells showed significant levels of fluorescence with the AAV5-based vector (n). Intense fluorescence was detected with the AAV5- and AAV8-based vectors in the inner sulcus cells (p and x). Scale bars: 10×, 100 μm; 20×, 50 μm; 40×, 25 μm; 60×, 25 μm.

doi:10.1016/j.ymthe.2005.03.021

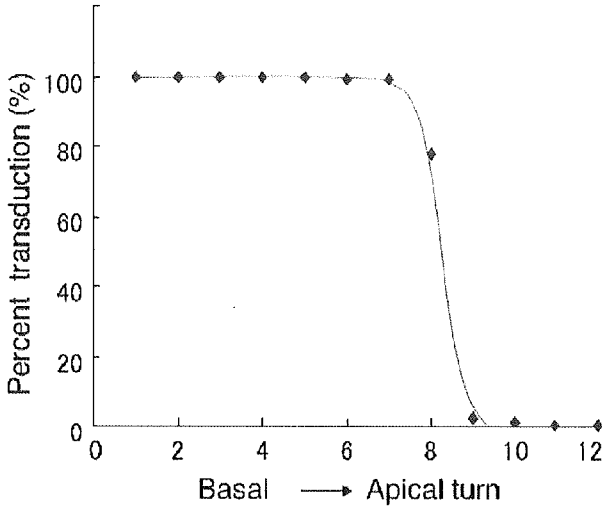

FIG. 4. EGFP expression profile of inner hair cells transduced with AAV3, as shown for a cross section subdivided into 12 segments ranging from the basal (high frequencies) to the apical (low frequencies) cochlear regions.

requires simple surgery without cochlear trauma [19]. Another critical factor in assessing the utility of a gene transfer vector is safety. Factors determining safety include the toxicity of the gene transfer agent itself, the provocation of immune responses, the generation of replication-competent virus, and the risk of creating genetically modified cells by insertional mutagenesis. The cells and tissues within the AAV-EGFP-perfused cochleae were free from inflammation and were generally intact. No pathological changes were observed in the organ of Corti, stria vascularis, or spiral ganglion cells. The long-term expression of EGFP within the cochlear tissues is consistent with data obtained from other animal models and different organ systems [9,33]. Since EGFP is known to introduce cellular toxicity, vectors expressing physiologically therapeutic proteins would achieve longer transduction periods than EGFP. Gene transfer into the inner hair cells presents numerous opportunities for auditory neuroscience. Potential applications include the localization of proteins by expression of tagged constructs, the generation of dominant-negative or antisense knockouts of endogenous proteins, the rescue of mutant phenotypes to identify disease genes, and perhaps even the treatment of auditory disorders. Advances in the molecular basis of auditory diseases have allowed the identification of a number of genetic disorders such as presbycusis, acoustic trauma, and ototoxicity. The development of gene therapy now allows us to evaluate the effects of transferring therapeutic genes into the inner ear by several different strategies. The expression of marker genes in the inner ear tissue has been demonstrated. Further studies will improve our understanding of cochlear function as well as provide for the development of novel therapies for a wide variety of inner ear diseases. Intracochlear gene transfer using AAV vectors has been established as a viable experimental proposition. Future study will include the transfer of functioning genes *in vivo* and the development of alternative vectors. While clinical application may be some way off, it is vital that gene delivery techniques are optimized in anticipation of future need.

In conclusion, the data presented in this paper demonstrate successful gene transfer into several types of cochlear cells *in vivo* with AAV-based vectors. Interestingly, the AAV3 vector promoted inner hair cell-specific transduction. These findings are of value for further molecular studies of the cochlear inner hair cells and for gene replacement strategies to correct hereditary hearing loss due to specific monogenic mutations affecting cochlear inner hair cells.

MATERIALS AND METHODS

Construction and preparation of proviral plasmids. The AAV vector proviral plasmid pAAV2-*LacZ* harbors an *Escherichia coli* β-galactosidase expression cassette with the CMV promoter, the first intron of the human growth hormone gene, and the SV40 early polyadenylation sequence, which are flanked by inverted terminal repeats (ITRs) [34]. The *LacZ* expression cassette of pAAV2-*LacZ* was ligated to *Not*I-excised pAAV5-RNL [35] to form the proviral plasmid pAAV5-*LacZ*. The pAAV2-CAG-EGFP-WPRE construct consists of the EGFP gene under the control of the CAG promoter (the chicken β-actin promoter associated with the cytomegalovirus immediate-early enhancer) and WPRE (woodchuck hepatitis virus posttranscriptional regulatory element) flanked by ITRs. The WPRE cassette augments the stability of transgene mRNA [36] and increases EGFP expression levels, thereby ensuring long-term transgene expression. A *Bam*HI–*Xba*I fragment containing the EGFP cDNA excised from pEGFP-1 and a *Hin*dIII fragment containing the WPRE sequence excised from pBS II SK$^+$WPRE-B11 (a gift from Dr. J. Donello) was ligated to *Xho*I linkers and cloned into an *Xho*I site of pCAGGS (a gift from Dr. J.-I. Miyazaki) to create pCAG-EGFP-WPRE. The EGFP expression cassette from pCAG-EGFP-WPRE was ligated to the *Not*I-excised pAAV2-*LacZ* and pAAV5-RNL [35] to form the proviral plasmids pAAV2-CAG-EGFP-WPRE and pAAV5-CAG-EGFP-WPRE, respectively. The AAV-helper plasmid harbors Rep and Cap. The adenovirus helper plasmid pAdeno5 (identical to pVAE2AE4-5) encodes the entire E2A and E4 regions and the VA RNA I and II genes [37]. Plasmids were purified with the Qiagen plasmid purification kits (Qiagen K.K., Tokyo, Japan).

Recombinant AAV vector production. Vectors derived from the AAV1–4, 7, and 8 pseudotypes were produced with the AAV packaging plasmid pAAV1RepCap (for AAV1) [38], pHLP19 (for AAV2), pAAV3RepCap (for AAV3) [39], pAAV4RepCap (for AAV4) [40], pAAV7RepCap (for AAV7) [41], or pAAV8RepCap (for AAV8) [41] and the AAV proviral plasmid pAAV2-*LacZ* or pAAV2-CAG-EGFP-WPRE. The plasmids pAAV5RepCap [35] and pAAV5-*LacZ*, or pAAV5-CAG-EGFP-WPRE, were used to produce vector with the AAV5 pseudotype [42]. Seven AAV serotype vectors were produced as previously described by the three-plasmid transfection adenovirus-free protocol [37]. Briefly, three days before transfection, 293 cells were plated onto a 10-tray Cell Factory (Nalge Nunc International, Rochester, NY, USA; 6×10^7 cells/10-tray). The cells were cotransfected with 650 μg each of the proviral plasmid, the AAV vector packaging plasmid, and the adenovirus helper plasmid pAdeno5 [34] by the calcium phosphate coprecipitation method. The medium was changed following incubation for 6–8 h at 37°C. Recombinant AAV was harvested 72 h after transfection by three freeze/thaw cycles. The crude viral lysate was purified twice on a cesium chloride two-tier centrifugation

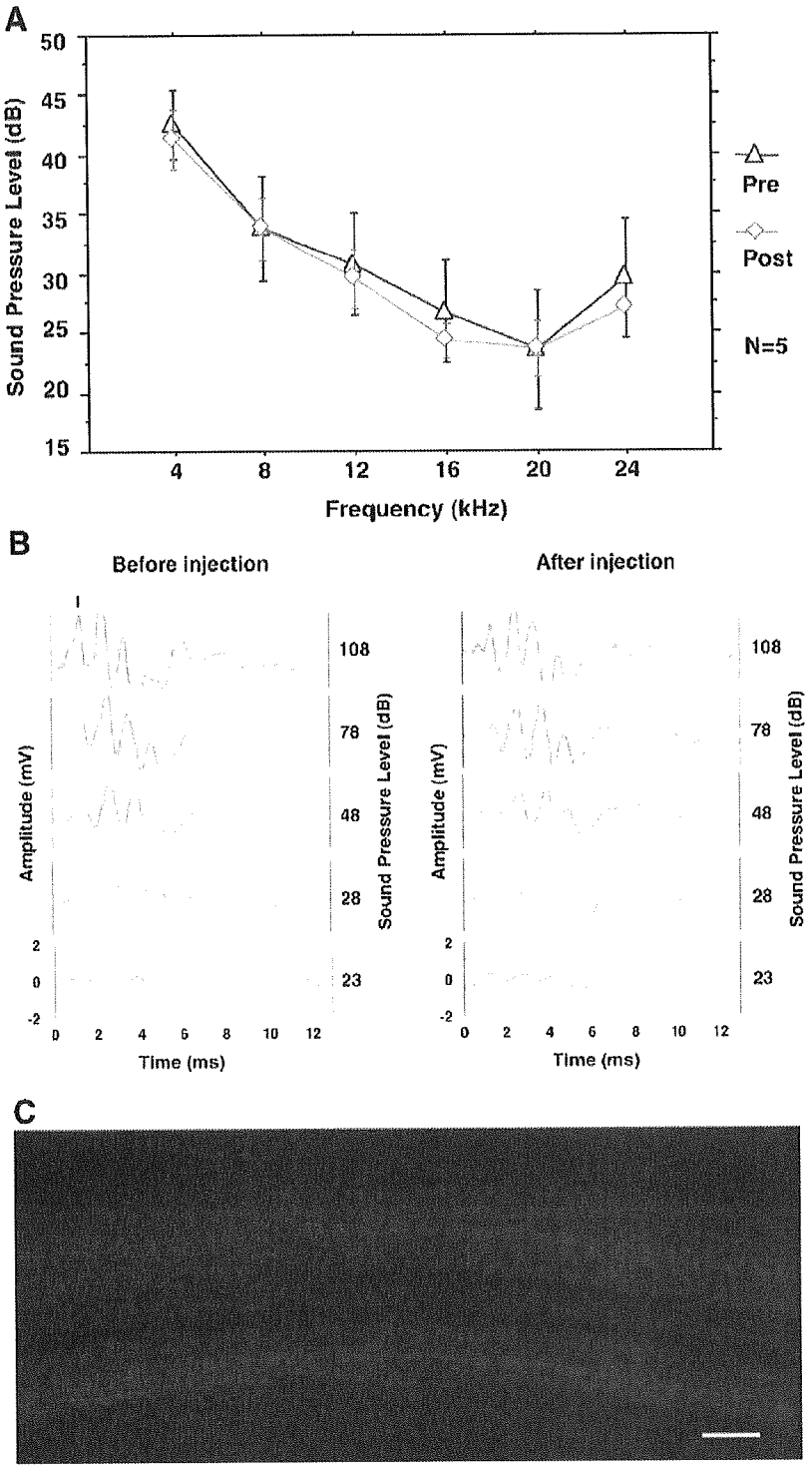

FIG. 5. (A) ABR threshold (mean ± SD) at each frequency tested preoperatively (pre) versus postoperatively (post). (B) Example of ABR waveforms in C57BL/6J at various stimuli (16 kHz; 108 dB, 78 dB, 48 dB, 28 dB, and 23 dB). ABR were tested in the transduced ear prior to viral injection and 10 days after injection. Wave I was measured to analyze the activity of the cochlea. (C) F-actin staining showing that no outer hair cells were lost from inoculated cochleae. Original magnification 40×; scale bar, 25 μm.

gradient as described previously [24]. The viral stock was treated with DNase and titrated by quantitative real-time PCR with plasmid standards [43].

Surgical procedures and cochlear perfusions. All animal studies were performed in accordance with the guidelines issued by the committee on animal research of Jichi Medical School and approved by its ethics

doi:10.1016/j.ymthe.2005.03.021

committee. Sixty female C57BL/6J mice (4 weeks of age; CLEA Japan, Tokyo, Japan) and 40 male ICR mice (2 months of age; Japan SLC, Shizuoka, Japan) were utilized. The mice were initially anesthetized with ketamine (50 mg/kg) and the analgesic xylazine (5 mg/kg). A postauricular approach was used to expose the tympanic bony bulla. A small opening (2 mm) in the tympanic bulla was carefully made to allow access to the round window membrane. In the tested groups, 5 μl AAV vector solution (5×10^{10} gc) was microinjected into the cochlea through the round window over 10 min with a glass micropipette (40 μm in diameter) fitted on a Univentor 801 syringe pump (Serial No. 170182, High Precision Instruments, Univentor Ltd., Malta) [19]. A small plug of muscle was used to seal the cochlea and the surgical wound was closed in layers and dressed with antibiotic ointment. Five mice of each strain received control cochlear perfusions with artificial perilymph (145 mM NaCl, 2.7 mM KCl, 2 mM $MgSO_4$, 1.2 mM $CaCl_2$, 5 mM Hepes) alone. Each AAV-EGFP serotype was injected into five mice of each strain. Another 20 C57BL/6J mice were injected with the AAV3 vector to study long-term expression.

Cochlear function assessment using ABR. To assess the physiological status of experimental ears, auditory thresholds were determined with multiple frequency and intensity tone bursts by performing ABR audiometry with Tucker–Davis Technologies and Scope v3.6.9 software (Power Lab/200; ADInstruments, Castle Hill, Australia). Tone pipes were introduced into the operated ears of the anesthetized mice, and evoked potentials were recorded using needle electrodes inserted through the skin. ABR were elicited and measured 256 times at 4, 8, 12, 16, 20, and 24 kHz frequencies with tone bursts in systematic 5-dB steps. The rise/fall times for the tone bursts were 0.1 ms rise/ms flat (cosine gate). Free-field system was used as a calibration procedure. Wave I was measured to analyze the activity from the cochlea. The lowest stimulus level that yielded a detectable ABR waveform was defined as the threshold. ABR were tested in the infused ear prior to surgery and 10 days postsurgery. Data were statistically analyzed using repeated-measures analysis of variance followed by paired Student's t test performed with StatView 5.0 software (SAS Institute Inc., Cary, NC, USA). Values of $P < 0.05$ were considered significant.

Histology. Cochlear transgene expression patterns were determined for all AAV serotypes by visualizing EGFP expression. The animals were sacrificed 10 days after injection, and intracardiac perfusion was performed with 4% paraformaldehyde (PFA) in 0.1 M phosphate buffer, pH 7.4. The cochleae were harvested and the stapes footplates were removed. For AAV3-mediated transduction, the animals (five mice for each time point) were sacrificed 1, 2, 4, 8, or 12 weeks after inoculation. Postfixation was carried out in 4% PFA for 4 h at 4°C, and decalcification was performed in 10% EDTA for 12 days at room temperature. The cochlear half-turns were microdissected and processed and the other half-turns were prepared by cryosection (10 μm) to detect EGFP expression by using an Olympus IX70 (Olympus Corp., Tokyo, Japan) fluorescence microscope with a standard fluorescein isothiocyanate filter set and Studio Lite software (Olympus Corp.). Cells that exhibited fluorescence were considered positive for transgene expression. The level of expression was graded by fluorescence intensity on a four-point scale (+, ++, +++, ++++) depending on the pixel/unit area count. Hair cell counts were carried out with dissected cochlea.

ACKNOWLEDGMENTS

The authors thank Avigen, Inc. (Alameda, CA, USA) for providing pAAV-LacZ, pHLP19, and pAdeno; Dr. John A. Chiorini for pAAV4RepCap (identical to pSV40oriAAV4-2), pAAV5-RNL, and pAAV5RepCap (identical to 5RepCapB); and Dr. James M. Wilson for pAAV7RepCap and pAAV8RepCap. We also thank Dr. John E. Donello (Infectious Disease Laboratory, The Salk Institute for Biological Studies) for providing pBS II SK+WPRE-B11 and Dr. Jun-Ichi Miyazaki (Osaka University Graduate School of Medicine) for pCAGGS. The authors also thank Mr. Takeshi Hayakawa (Bio Research Center Co., Ltd.), Ms. Miyoko Mitsu, and Ms. Kiyomi Aoki for their encouragement and technical support. This study was supported in part by (1) grants from the Ministry of Health, Labor, and Welfare of Japan; (2) Grants-in-Aid for Scientific Research; (3) a grant from the 21 Century COE Program; and (4) the High-Tech Research Center Project for Private Universities matching fund subsidy from the Ministry of Education, Culture, Sports, Science, and Technology of Japan.

RECEIVED FOR PUBLICATION NOVEMBER 1, 2004; ACCEPTED MARCH 24, 2005.

REFERENCES

1. Raphael, Y., Frisancho, J. C., and Roessler, B. J. (1996). Adenoviral-mediated gene transfer into guinea pig cochlear cells in vivo. *Neurosci. Lett.* **207:** 137–141.
2. Holt, J. R., *et al.* (1999). Functional expression of exogenous proteins in mammalian sensory hair cells infected with adenoviral vectors. *J. Neurophysiol.* **81:** 1881–1888.
3. Yamasoba, T., Suzuki, M., and Kondo, K. (2002). Transgene expression in mature guinea pig cochlear cells in vitro. *Neurosci. Lett.* **335:** 13–16.
4. Derby, M. L., Sena-Esteves, M., Breakefield, X. O., and Corey, D. P. (1999). Gene transfer into the mammalian inner ear using HSV-1 and vaccinia virus vectors. *Hear. Res.* **134:** 1–8.
5. Chen, X., Frisina, R. D., Bowers, W. J., Frisina, D. R., and Federoff, H. J. (2001). HSV amplicon-mediated neurotrophin-3 expression protects murine spiral ganglion neurons from cisplatin-induced damage. *Mol. Ther.* **3:** 958–963.
6. Bowers, W. J., Chen, X., Guo, H., Frisina, D. R., Federoff, H. J., and Frisina, R. D. (2002). Neurotrophin-3 transduction attenuates cisplatin spiral ganglion neuron ototoxicity in the cochlea. *Mol. Ther.* **6:** 12–18.
7. Han, J. J., *et al.* (1999). Transgene expression in the guinea pig cochlea mediated by a lentivirus-derived gene transfer vector. *Hum. Gene Ther.* **10:** 1867–1873.
8. Lalwani, A. K., Walsh, B. J., Reilly, P. G., Muzyczka, N., and Mhatre, A. N. (1996). Development of in vivo gene therapy for hearing disorders: introduction of adeno-associated virus into the cochlea of the guinea pig. *Gene Ther.* **3:** 588–592.
9. Lalwani, A., *et al.* (1998). Long-term in vivo cochlear transgene expression mediated by recombinant adeno-associated virus. *Gene Ther.* **5:** 277–281.
10. Luebke, A. E., Foster, P. K., Muller, C. D., and Peel, A. L. (2001). Cochlear function and transgene expression in the guinea pig cochlea, using adenovirus- and adeno-associated virus-directed gene transfer. *Hum. Gene Ther.* **12:** 773–781.
11. Luebke, A. E., Steiger, J. D., Hodges, B. L., and Amalfitano, A. (2001). A modified adenovirus can transfect cochlear hair cells in vivo without compromising cochlear function. *Gene Ther.* **8:** 789–794.
12. Staecker, H., Li, D., O'Malley, B. W., Jr., and Van De Water, T. R. (2001). Gene expression in the mammalian cochlea: a study of multiple vector systems. *Acta Otolaryngol.* **121:** 157–163.
13. Dazert, S., Aletsee, C., Brors, D., Gravel, C., Sendtner, M., and Ryan, A. (2001). In vivo adenoviral transduction of the neonatal rat cochlea and middle ear. *Hear. Res.* **151:** 30–40.
14. Ishimoto, S., Kawamoto, K., Kanzaki, S., and Raphael, Y. (2002). Gene transfer into supporting cells of the organ of Corti. *Hear. Res.* **173:** 187–197.
15. Van de Water, T. R., Staecker, H., Halterman, M. W., and Federoff, H. J. (1999). Gene therapy in the inner ear: mechanisms and clinical implications. *Ann. N.Y. Acad. Sci.* **884:** 345–360.
16. Vassalli, G., Bueler, H., Dudler, J., von Segesser, L. K., and Kappenberger, L. (2003). Adeno-associated virus (AAV) vectors achieve prolonged transgene expression in mouse myocardium and arteries in vivo: a comparative study with adenovirus vectors. *Int. J. Cardiol.* **90:** 229–238.
17. Li Duan, M., Bordet, T., Mezzina, M., Kahn, A., and Ulfendahl, M. (2002). Adenoviral and adeno-associated viral vector mediated gene transfer in the guinea pig cochlea. *Neuroreport* **13:** 1295–1299.
18. Lalwani, A. K., Han, J. J., Walsh, B. J., Zolotukhin, S., Muzyczka, N., and Mhatre, A. N. (1997). Green fluorescent protein as a reporter for gene transfer studies in the cochlea. *Hear. Res.* **114:** 139–147.
19. Kho, S. T., Pettis, R. M., Mhatre, A. N., and Lalwani, A. K. (2000). Cochlear microinjection and its effects upon auditory function in the guinea pig. *Eur. Arch. Otorhinolaryngol.* **257:** 469–472.
20. Handa, A., Muramatsu, S., Qiu, J., Mizukami, H., and Brown, K. E. (2000). Adeno-associated virus (AAV)-3-based vectors transduce haematopoietic cells not susceptible to transduction with AAV-2-based vectors. *J. Gen. Virol.* **81:** 2077–2084.
21. Davidson, B. L., *et al.* (2000). Recombinant adeno-associated virus type 2, 4, and 5 vectors: transduction of variant cell types and regions in the mammalian central nervous system. *Proc. Natl. Acad. Sci. USA* **97:** 3428–3432.
22. Zabner, J., *et al.* (2000). Adeno-associated virus type 5 (AAV5) but not AAV2 binds to the apical surfaces of airway epithelia and facilitates gene transfer. *J. Virol.* **74:** 3852–3858.
23. Yang, G. S., *et al.* (2002). Virus-mediated transduction of murine retina with adeno-associated virus: effects of viral capsid and genome size. *J. Virol.* **76:** 7651–7660.
24. Okada, T., *et al.* (2002). Adeno-associated virus vectors for gene transfer to the brain. *Methods* **28:** 237–247.
25. Xu, L., *et al.* (2001). CMV-beta-actin promoter directs higher expression from an

adeno-associated viral vector in the liver than the cytomegalovirus or elongation factor 1 alpha promoter and results in therapeutic levels of human factor X in mice. *Hum. Gene Ther.* **12:** 563–573.
26. Chung, S., Andersson, T., Sonntag, K. C., Bjorklund, L., Isacson, O., and Kim, K. S. (2002). Analysis of different promoter systems for efficient transgene expression in mouse embryonic stem cell lines. *Stem Cells* **20:** 139–145.
27. Nomoto, T., *et al.* (2003). Distinct patterns of gene transfer to gerbil hippocampus with recombinant adeno-associated virus type 2 and 5. *Neurosci. Lett.* **340:** 153–157.
28. Dutta, S. K. (1975). Isolation and characterization of an adenovirus and isolation of its adenovirus-associated virus in cell culture from foals with respiratory tract disease. *Am. J. Vet. Res.* **36:** 247–250.
29. Palmer, E., and Goldsmith, C. S. (1988). Ultrastructure of human retroviruses. *J. Electron Microsc. Tech.* **8:** 3–15.
30. Stover, T., Yagi, M., and Raphael, Y. (1999). Cochlear gene transfer: round window versus cochleostomy inoculation. *Hear. Res.* **136:** 124–130.
31. Stover, T., Yagi, M., and Raphael, Y. (2000). Transduction of the contralateral ear after adenovirus-mediated cochlear gene transfer: round window versus cochleostomy inoculation. *Gene Ther.* **7:** 377–383.
32. Kawamoto, K., Oh, S. H., Kanzaki, S., Brown, N., and Raphael, Y. (2001). The functional and structural outcome of inner ear gene transfer via the vestibular and cochlear fluids in mice. *Mol. Ther.* **4:** 575–585.
33. Kaplitt, M. G., *et al.* (1994). Long-term gene expression and phenotypic correction using adeno-associated virus vectors in the mammalian brain. *Nat. Genet.* **8:** 148–154.
34. Okada, T., *et al.* (2001). Development and characterization of an antisense-mediated prepackaging cell line for adeno-associated virus vector production. *Biochem. Biophys. Res. Commun.* **288:** 62–68.
35. Chiorini, J. A., Kim, F., Yang, L., and Kotin, R. M. (1999). Cloning and characterization of adeno-associated virus type 5. *J. Virol.* **73:** 1309–1319.
36. Zufferey, R., Donello, J. E., Trono, D., and Hope, T. J. (1999). Woodchuck hepatitis virus posttranscriptional regulatory element enhances expression of transgenes delivered by retroviral vectors. *J. Virol.* **73:** 2886–2892.
37. Matsushita, T., *et al.* (1998). Adeno-associated virus vectors can be efficiently produced without helper virus. *Gene Ther.* **5:** 938–945.
38. Mochizuki, S., *et al.* (2004). Adeno-associated virus (AAV) vector-mediated liver- and muscle-directed transgene expression using various kinds of promoters and serotypes. *Gene Ther. Mol. Biol.* **8:** 9–18.
39. Muramatsu, S., Mizukami, H., Young, N. S., and Brown, K. E. (1996). Nucleotide sequencing and generation of an infectious clone of adeno-associated virus 3. *Virology* **221:** 208–217.
40. Chiorini, J. A., Yang, L., Liu, Y., Safer, B., and Kotin, R. M. (1997). Cloning of adeno-associated virus type 4 (AAV4) and generation of recombinant AAV4 particles. *J. Virol.* **71:** 6823–6833.
41. Gao, G. P., Alvira, M. R., Wang, L., Calcedo, R., Johnston, J., and Wilson, J. M. (2002). Novel adeno-associated viruses from rhesus monkeys as vectors for human gene therapy. *Proc. Natl. Acad. Sci. USA* **99:** 11854–11859.
42. Rabinowitz, J. E., *et al.* (2002). Cross-packaging of a single adeno-associated virus (AAV) type 2 vector genome into multiple AAV serotypes enables transduction with broad specificity. *J. Virol.* **76:** 791–801.
43. Veldwijk, M. R., *et al.* (2002). Development and optimization of a real-time quantitative PCR-based method for the titration of AAV-2 vector stocks. *Mol. Ther.* **6:** 272–278.
44. Kikuchi, T., *et al.* (1995). *Anat. Embryol. (Berlin)* **191:** 101–118.

ARTICLE

doi:10.1016/j.ymthe.2005.08.009

Viral-Mediated Temporally Controlled Dopamine Production in a Rat Model of Parkinson Disease

Xiao-gang Li,[1,2] Takashi Okada,[2] Mika Kodera,[1] Yuko Nara,[1] Naomi Takino,[1] Chieko Muramatsu,[1] Kunihiko Ikeguchi,[1] Fumi Urano,[3] Hiroshi Ichinose,[3] Daniel Metzger,[4] Pierre Chambon,[4] Imaharu Nakano,[1] Keiya Ozawa,[2,*] and Shin-ichi Muramatsu[1,†]

[1]*Division of Neurology, Department of Medicine, and* [2]*Divison of Genetic Therapeutics, Center for Molecular Medicine, Jichi Medical School, Tochigi 329-0498, Japan*

[3]*Department of Life Science, Tokyo Institute of Technology, Kanagawa 226-8501, Japan*

[4]*Institut de Génétique et de Biologie Moléculaire et Cellulaire, Centre National de la Recherche Scientifique, Institut National de la Santé et de la Recherche Médicale, Université Louis Pasteur, Collège de France, and Institut Clinique de la Souris, 67404 Illkirch Cedex, France*

**To whom correspondence and reprint requests should be addressed at the Division of Genetic Therapeutics, Center for Molecular Medicine, Jichi Medical School, 3311-1 Yakushiji, Minamikawachi, Tochigi 329-0498, Japan. Fax: +81 285 44 8675. E-mail: kozawa@ms.jichi.ac.jp.*

†To whom correspondence and reprint requests should be addressed at the Division of Neurology, Department of Medicine, Jichi Medical School, 3311-1 Yakushiji, Minamikawachi, Tochigi 329-0498, Japan. Fax: +81 285 44 5118. E-mail: muramats@ms.jichi.ac.jp.

Available online 22 September 2005

Regulation of gene expression is necessary to avoid possible adverse effects of gene therapy due to excess synthesis of transgene products. To reduce transgene expression, we developed a viral vector-mediated somatic regulation system using inducible Cre recombinase. A recombinant adeno-associated virus (AAV) vector expressing Cre recombinase fused to a mutated ligand-binding domain of the estrogen receptor α (CreER^{T2}) was delivered along with AAV vectors expressing dopamine-synthesizing enzymes to rats of a Parkinson disease model. Treatment with 4-hydroxytamoxifen, a synthetic estrogen receptor modulator, activated Cre recombinase within the transduced neurons and induced selective excision of the tyrosine hydroxylase (TH) coding sequence flanked by loxP sites, leading to a reduction in transgene-mediated dopamine synthesis. Using this strategy, aromatic L-amino acid decarboxylase (AADC) activity was retained so that L-3,4-dihydroxyphenylalanine (L-dopa), a substrate for AADC, could be converted to dopamine in the striatum and the therapeutic effects of L-dopa preserved, even after reduction of TH expression in the case of dopamine overproduction. Our data demonstrate that viral vector-mediated inducible Cre recombinase can serve as an *in vivo* molecular switch, allowing spatial and temporal control of transgene expression, thereby potentially increasing the safety of gene therapy.

Key Words: adeno-associated virus, gene therapy, gene regulation, tamoxifen, Cre recombinase, Parkinson disease, dopamine

INTRODUCTION

Advances in gene transfer methods, in particular the development of improved viral vectors, have expanded the potential of gene therapy to treat a wide range of genetic and acquired diseases. Efficient and long-term expression of therapeutic genes within the central nervous system has been demonstrated in preclinical studies aimed at treating neurodegenerative disorders, including Parkinson disease (PD) [1,2]. PD is a progressive movement disorder characterized by selective degeneration of dopaminergic neurons within the substantia nigra, which project to the striatum. As the dopamine content of the striatum decreases severely, its replacement becomes an important strategy to alleviate motor impairment of the disease. One such strategy is gene therapy to restore the local production of dopamine. Recombinant adeno-associated virus (AAV) vector-mediated gene transfer of dopamine-synthesizing enzymes, such as tyrosine hydroxylase (TH) and guanosine triphosphate cyclohydrolase I (GCH), with or without aromatic L-amino acid decarboxylase (AADC), has induced behavioral recovery in animal models of PD [3–5]. Before clinical trials examining this therapy can commence, however, it is desirable to have a mechanism by which

1525-0016/$30.00

dopamine synthesis can be controlled by regulation of gene expression.

Methods utilizing the properties of bacteriophage P1 site-specific Cre recombinase have been developed in recent years as a means of generating somatic mutations [6]. Regulation of Cre recombinase activity, achieved by fusing Cre with mutated hormone-binding domains of various steroid receptors, has been used in various transgenic applications [7,8]. A chimeric protein known as CreER^{T2}, obtained by fusing Cre to a mutated ligand binding domain of the human estrogen receptor α, is particularly useful. Cell-specific expression of CreER^{T2} in transgenic mice allows efficient tamoxifen-dependent Cre-mediated recombination at loci flanked by loxP sites, without background activity [9]. In the present study, we demonstrate that stereotaxic injection of recombinant AAV vectors expressing dopamine-synthesizing enzymes and CreER^{T2} enables spatiotemporal control of dopamine levels within the brains of rats of a PD model. Our results indicate that these vectors may have a number of applications in gene therapy.

RESULTS

Viral-Mediated Temporally Controlled Cre-Mediated Recombination

We generated AAV vectors expressing either Cre recombinase containing a nuclear localization signal (AAV-Cre) or tamoxifen-dependent Cre recombinase (AAV-CreER^{T2}). To engineer a reporter system, we designed an AAV-EGFP/Red vector to express a destabilized variant of red fluorescent protein (DsRed-Express DR) only after Cre-mediated recombination of a loxP-flanked DNA segment encoding a destabilized, red-shifted variant of green fluorescent protein (d2EGFP) (Fig. 1A). To determine the efficacy of viral-mediated recombination, we infected HEK293 cells with AAV-EGFP/Red and either AAV-Cre or AAV-CreER^{T2} (Fig. 1B). Co-infection of AAV-Cre and AAV-EGFP/Red resulted in expression of DsRed-Express-DR, while only d2EGFP was expressed in control cells infected with AAV-EGFP/Red alone. Co-infection with the reporter vector and AAV-CreER^{T2} induced DsRed-Express-DR expression in almost all 4-hydroxytamoxifen (4-OHT)-treated cells. Although we detected slight background expression of DsRed-Express-DR in the absence of 4-OHT, we observed only a limited number of these cells (<1%), indicating that CreER^{T2} activity is tightly regulated in these virally transduced cells. To test the potential use of AAV-CreER^{T2} *in vivo*, we used stereotaxic injections to deliver AAV-CreER^{T2} into the brains of reporter mice [10]. These mice were engineered to express a red-shifted variant of the wild-type green fluorescent protein (EGFP) only after Cre-mediated excision of a loxP DNA fragment. After 5 consecutive days of 4-OHT treatment (1 mg by intraperitoneal injection), we observed numerous EGFP-expressing cells in AAV-injected brains, all of which coexpressed Cre recombinase (Fig. 1C). In the absence of treatment with 4-OHT, only a few cells (<0.1% of Cre-positive cells) expressed EGFP in the vicinity of AAV-CreER^{T2}-injected sites (data not shown). These data indicate that floxed DNA segments are efficiently excised *in vivo* by combining AAV-CreER^{T2} injection with 4-OHT treatment.

Temporally Controlled Reduction of Dopamine Synthesis

We generated AAV vectors expressing each of the three dopamine-synthesizing enzymes (TH, AADC, and GCH). In the TH-expressing vector, two loxP sites flanked the TH coding sequence (AAV-floxed TH). We infected HEK293 cells with these dopamine-synthesizing vectors (AAV-floxed TH, AAV-AADC, and AAV-GCH) in combination

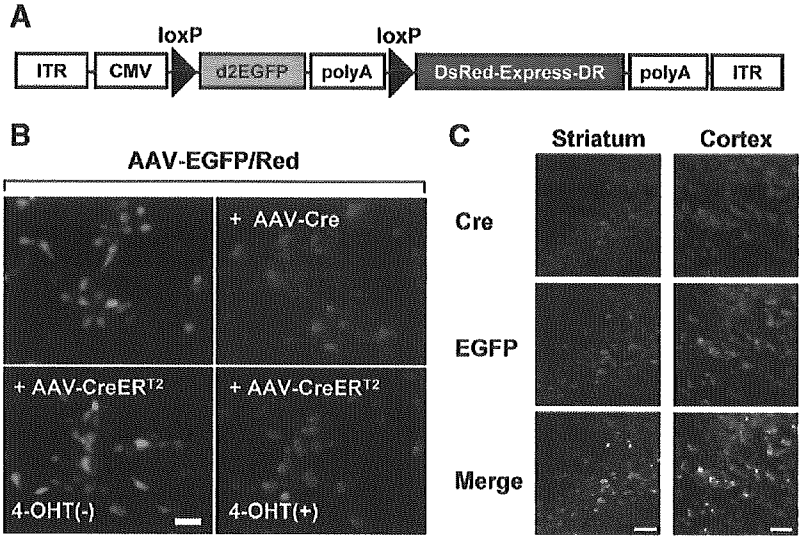

FIG. 1. Viral vector-mediated Cre-dependent floxed DNA excision. (A) Illustration of the AAV-EGFP/Red vector construct. A DsRed-Express-DR marker was placed downstream of the d2EGFP marker with a SV40 poly(A) sequence flanked by loxP sites. ITR, inverted terminal repeat; CMV, human cytomegalovirus immediate-early promoter followed by the first intron of human growth hormone. (B) 4-OHT-induced Cre-dependent recombination. HEK293 cells were infected with AAV-EGFP/Red and either AAV-Cre or AAV-CreER^{T2}. 4-OHT was added to the medium 5 h after infection. Fluorescence was observed 48 h after infection. Bar, 40 μm. (C) EGFP expression in the AAV-CreER^{T2}-injected striatum and cortex of transgenic mice. 4-OHT (1 mg) was administered intraperitoneally 1 week after vector injection every day for 5 days until the mice were killed. In these mice, the stop fragment was flanked by loxP sites and placed between the EGFP sequence and the *Gt(ROSA)26Sor* promoter. Bar, 40 μm.

doi:10.1016/j.ymthe.2005.08.009

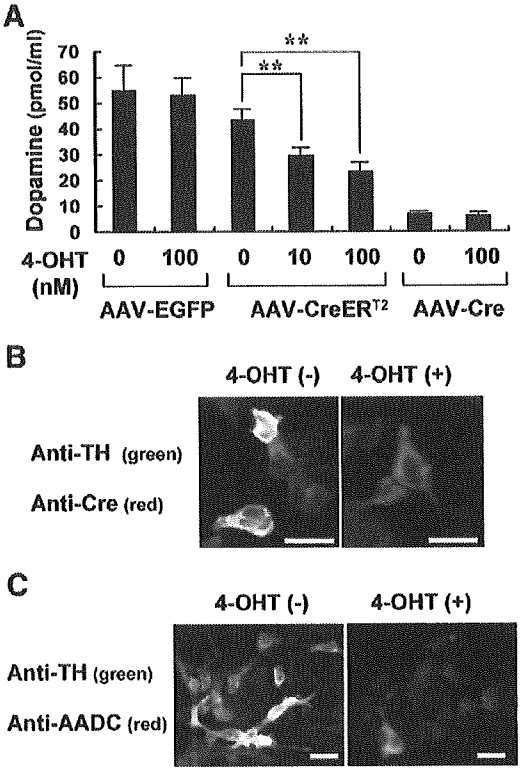

FIG. 2. Reduced dopamine synthesis after 4-OHT-induced ablation of a floxed TH transgene. HEK293 cells were infected with dopamine-synthesizing vectors (AAV-floxed TH, AAV-AADC, and AAV-GCH) in combination with AAV-CreER^{T2} or control vectors. (A) Dopamine content in the culture medium was significantly reduced in the presence of 4-OHT. $^{**}P < 0.01$, $n = 4$. (B) TH (green) and CreER^{T2} (red) immunocytochemistry was performed 48 h after vector infection. Yellow fluorescence in the merged image indicates colocalization. In the presence of 4-OHT, CreER^{T2} translocated to the nucleus. TH was not expressed in cells positive for nuclear CreER^{T2}. Bar, 20 μm. (C) TH (green) and AADC (red) immunocytochemistry. Note the reduced number of TH-positive cells in the presence of 4-OHT. Bar, 20 μm.

with AAV-CreER^{T2} or control vectors. We found that treatment with 4-OHT significantly reduced dopamine synthesis (Fig. 2A). Immunocytochemistry demonstrated coexpression of TH and CreER^{T2} in the cytoplasm in the absence of 4-OHT and an absence of TH expression when CreER^{T2} was translocated into the nucleus in the presence of 4-OHT (Fig. 2B). The expression of AADC was not reduced by the presence of 4-OHT (Fig. 2C). Dual labeling showed that more than 80% of the TH-immunoreactive (TH-IR) cells were also positive for AADC (251 of 300) and Cre (242 of 300) in the absence of 4-OHT-treatment.

Reduction of Dopamine Production in a Rat Model

We next tested whether the vector-mediated Cre-dependent regulation of transgene expression observed in culture could be extended to animal models. We obtained hemiparkinsonian rats by injecting a selective neurotoxin, 6-hydroxydopamine (6-OHDA), into the left medial forebrain bundle. The animals then received a mixture of AAV-CreER^{T2}, AAV-floxed TH, AAV-AADC, and AAV-GCH into their lesioned striatum, after which two-thirds were further treated with 4-OHT (4 mg/kg by intraperitoneal injection for 5 days) during the course of experimentation. Control rats were injected with AAV-LacZ alone or with AAV-Cre plus AAV-floxed TH, AAV-AADC, and AAV-GCH. To evaluate abnormal motor functions associated with depletion of dopamine in the striatum, we repeated quantification of apomorphine-induced rotation, as well

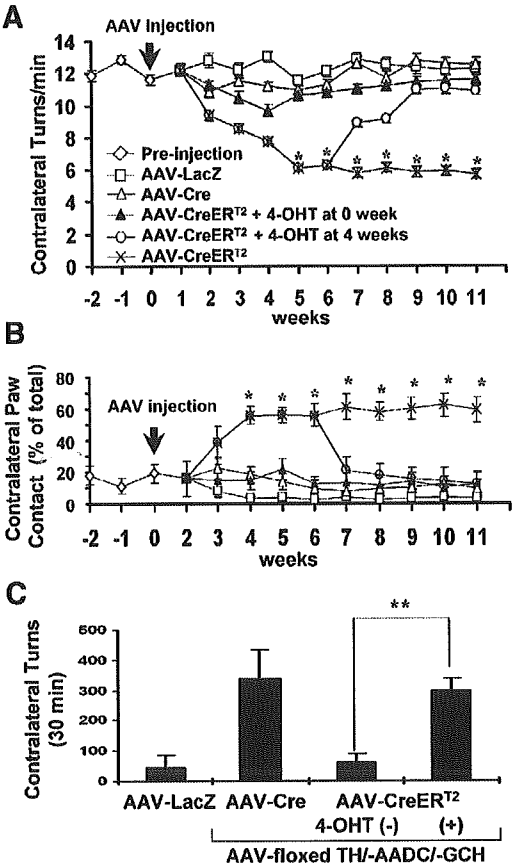

FIG. 3. Temporal control of dopamine synthesis in a rat model of PD transduced with AAV vectors. Sixty hemiparkinsonian rats were generated by 6-OHDA injection. Thirty-six received a mixture of AAV-CreER^{T2}, AAV-floxed TH, AAV-AADC, and AAV-GCH, after which they were divided into three groups of 12. Two of the groups were treated with 4-OHT (4 mg/kg by intraperitoneal injection for 5 days), at the same time or 4 weeks after vector injection. Control PD rats were injected with AAV-LacZ alone ($n = 12$) or AAV-Cre ($n = 12$), instead of AAV-CreER^{T2} with AAV-floxed TH, AAV-AADC, and AAV-GCH. (A) The total number of complete body turns induced by apomorphine was counted for each rat, and (B) spontaneous limb use was scored using the cylinder test. $^{*}P < 0.05$. (C) Efficient conversion of L-dopa to dopamine by AADC. L-Dopa (5 mg/kg) was administered to 4-OHT-treated rats and AAV-Cre-injected rats. Contralateral turning in response to L-dopa was counted for 30 min. $^{**}P < 0.01$. Legend symbols are as shown in A and B.

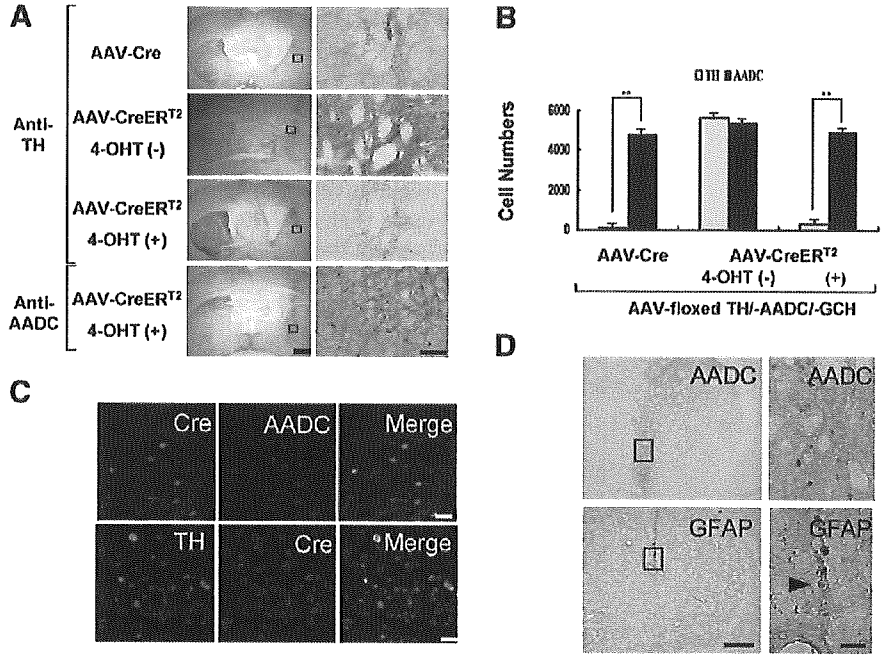

FIG. 4. Selective ablation of the TH transgene induced by treatment with 4-OHT. (A) Immunohistochemical staining for TH or AADC in the brains of 6-OHDA-lesioned rats 12 weeks after stereotaxic injection of AAV-Cre or AAV-CreER^{T2}, with or without 4-OHT treatment. AAV vectors were injected into the lesioned side of the striatum (right side of the photos). High-power-magnified images of the vector injection sites (squares in the left column) are shown in the right column. Representative photographs are also shown. Bar, 1.5 mm (left column), 100 μm (right column). (B) Number of immunoreactive (IR) cells against TH or AADC in the multiple AAV vector-injected striatum. The number of cells in 11 sections per rat (n = 3 for each group) was counted. The numbers of TH-IR cells and AADC-IR cells in AAV-CreER^{T2}-injected rats given 4-OHT 0 or 4 weeks after vector injection were indistinguishable and the results pooled for comparison with other groups. $^{**}P < 0.01$. (C) Efficient cotransduction of AAV vectors, as determined by dual immunofluorescence staining of the 6-OHDA-lesioned striatum. The majority of Cre-IR cells were also positive for TH and AADC. Bar, 20 μm. (D) Parallel striatal sections immunostained for glial fibrillary acidic protein (GFAP) or AADC. Striatal cells were transduced without obvious reactive astrocytosis. Residual hemosiderin was observed along the needle tract. On the right are magnified views of the boxes on the left. Bars: 0.5 mm, left; 50 μm, right.

as the cylinder test, weekly until the rats were killed. In the absence of 4-OHT, we observed behavioral recovery in rats that received both AAV-CreER^{T2} and AAV vectors expressing dopamine-synthesizing enzymes. Following 4-OHT treatment, these rats regressed, demonstrating impaired behavior (Figs. 3A and 3B). No recovery occurred in AAV-CreER^{T2}-injected rats treated with 4-OHT at the same time as vector injection or in AAV-Cre- or AAV-LacZ-injected rats. Contralateral turning in response to L-3,4-dihydroxyphenylalanine (L-dopa, 5 mg/kg) was not significantly reduced in 4-OHT-treated rats or AAV-Cre injected rats, indicating efficient conversion of L-dopa to dopamine in the striatum due to preservation of AADC activity (Fig. 3C).

Immunohistochemistry showed fewer TH-IR cells in rats that received AAV-Cre or AAV-CreER^{T2} plus 4-OHT, compared to injected rats not treated with 4-OHT (Figs. 4A and 4B). The numbers of AADC-immunoreactive cells,

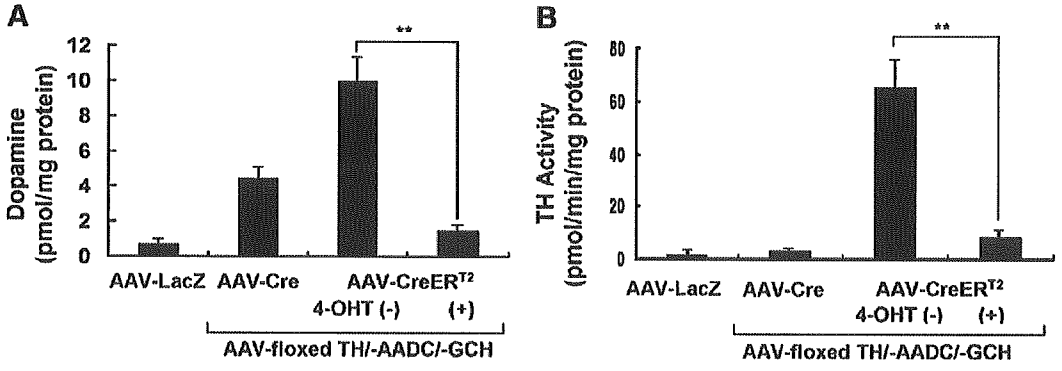

FIG. 5. Reduction of dopamine synthesis in 4-OHT-treated rats. Significantly less (A) dopamine content and (B) TH activity were observed in the lesioned striatum of 4-OHT-treated rats 12 weeks after vector injection, compared to 4-OHT-untreated rats. $^{**}P < 0.01$, n = 4.

doi:10.1016/j.ymthe.2005.08.009

however, did not differ significantly between 4-OHT-treated and untreated rats. We roughly estimated the number of transduced cells in the striatum at 5×10^4 based on cell counts performed on the tissue sections. This efficiency of transduction is sufficient to parallel the functional effects on behavior observed in other studies [3,5,11]. Double-labeling with both anti-Cre and anti-TH antibodies, or with anti-Cre and anti-AADC antibodies, showed that more than 80% of Cre-immunoreactive cells were also positive for TH (164 of 200) and AADC (176 of 200) in three 4-OHT-untreated rats (Fig. 4C). Immunostaining for glial fibrillary acidic protein (GFAP) or AADC in parallel sections demonstrated transduction of striatal cells without obvious reactive astrocytosis (Fig. 4D). Dopamine content (Fig. 5A) and TH activity (Fig. 5B) within the lesioned striatum were significantly lower in 4-OHT-treated compared to untreated rats. Dopamine levels in the transduced striatum in the 4-OHT-treated and untreated rats were 0.66 and 4.3%, respectively, those of the unlesioned striatum. Unlike primary dopamine in the nigrostriatal system, which is stored in synaptic vesicles, genetically produced dopamine in the lesioned striatum might be readily metabolized without storage. Since the dopamine level in the lesioned side of AAV-LacZ-injected rats was much lower (0.3%), a 10-fold increase in dopamine level after triple transduction with TH, AADC, and GCH genes caused a remarkable therapeutic effect. Average TH activity, measured in terms of L-dopa production (pmol/min/mg protein), reached 51.6% that of the normal striatum (65.9 ± 11.0 versus 127.7 ± 3.7) in rats transduced with dopamine-synthesizing enzymes. In 4-OHT-treated rats, TH activity fell to 10.8% of normal (13.8 ± 4.1).

Discussion

Our results show efficient viral vector-mediated delivery of tamoxifen-dependent CreER^{T2} recombinase into rodent brains and that transgenic floxed sequences can be deleted in a temporally controlled manner. In a rat model of PD, recombinant AAV vector-mediated delivery of CreER^{T2} into the striatum enabled 4-OHT-induced excision of a floxed TH transgene, resulting in reduced virally mediated dopamine synthesis. We targeted TH, a rate-limiting enzyme for dopamine biosynthesis that converts dietary L-tyrosine to L-dopa. Using this strategy, AADC activity was retained so that L-dopa, a substrate for AADC capable of crossing the blood–brain barrier, could be converted to dopamine in the striatum. Thus, in clinical situations, the therapeutic effects of orally administered L-dopa would likely be preserved, even after 4-OHT treatment to reduce TH expression in cases of dopamine overproduction [11]. Although transduction with AADC alone, in combination with oral administration of L-dopa, might not achieve continuous delivery of L-dopa, in contrast to that which could potentially be achieved with triple transduction of TH, AADC, and GCH, dopamine production could be regulated by altering the dose of L-dopa, thereby providing a safer option for gene therapy. We previously demonstrated that dopamine synthesis was enhanced (greater than fivefold) after systemic administration of L-dopa in AAV-TH/-AADC/-GCH-injected striatum in the primate model of PD using *in vivo* dialysis [4]. A phase I clinical trial involving gene transfer of AADC alone is currently under way.

AAV vectors are powerful tools by which to deliver therapeutic genes into the mammalian brain. Many striatal neurons of rodents and nonhuman primates are transduced with AAV vectors via stereotaxic injection, and long-term gene expression has been achieved without substantial toxicity or immune response [2,12]. AAV vectors have safety advantages over other viral vectors when it comes to *in vivo* gene delivery, since they are derived from nonpathogenic wild-type viruses. Moreover, most recombinant AAVs are present in cells as episomes, thus reducing the probability of insertional activation of oncogenes, compared to retroviruses, which integrate into host chromosomes [13]. Although it is difficult to use a single AAV vector for multiple gene transfer due to its limited packaging capacity (<5 kb), a single cell can be simultaneously transduced with multiple AAV vectors. In the present study, dual immunofluorescence staining showed efficient cotransduction of cells with different AAV vectors in the rat striatum, a finding consistent with that which we observed in a previous study [5].

Gene therapy strategies for the treatment of PD using AAV vectors include gene delivery of dopamine-synthesizing enzymes into the striatum to restore dopamine production, as well as gene delivery of neuroprotective molecules, such as glial cell line-derived neurotrophic factor, to block or slow down further degeneration [14]. In addition, AAV vectors harboring genes encoding neurotrophic factors might be delivered by intramuscular administration in an attempt to protect spinal motoneurons in patients suffering from amyotrophic lateral sclerosis [15–17]. Although no adverse effects due to overexpression of transgenes have been reported in animals to date, it is necessary to develop vectors that allow for regulation of transgene expression, thus avoiding transgene overexpression. In PD, overproduction of dopamine has the potential to cause dyskinesia or hallucinations, and sustained exposure to high concentrations of neurotrophic factors could result in tumor formation.

Inducible Cre recombinases have been used to generate a number of conditional knockout mice. They are invaluable tools for investigators studying the role of gene function in development, as well as a number of physiological and pathological processes. The tamoxifen-dependent CreER^{T2} recombinase has proven particularly helpful [9,18,19]. It has been shown that 4-OHT does not alter dopamine content within the striatum in mice [20],

and we did not observe any adverse effects of 4-OHT treatment in the present experiment. In addition, tamoxifen, which is metabolized by the liver into 4-OHT, has neuroprotective effects [21,22]. Thus, the CreER^{T2} system might be useful for gene therapy in the treatment of neurological diseases.

We have expanded upon the use of inducible Cre recombinase technology to regulate transgene expression using an AAV vector-mediated gene delivery system. Recently, a viral vector-mediated RNA interference (RNAi) approach has been developed and localized gene knockdown achieved in the adult brain [23–25]. Although RNAi-mediated suppression of gene function has a wide variety of applications, more specific and inducible transgene silencing can be achieved with AAV-CreER^{T2}. Selective ablation of floxed transgenes reduces the possibility of down-regulation of normal cellular proteins. This system works as a molecular switch, increasing the safety of long-acting gene therapy by avoiding or minimizing side effects due to overproduction of the protein product and by providing the ability to shut down expression if toxicities are encountered or treatment is completed. The ability to restrict somatic recombination of transgenes spatially and temporally has a wide range of applications, in both gene therapy and biological study requiring somatic genetic manipulation.

Materials and Methods

AAV vector production. The AAV vector plasmids contained an expression cassette with a human cytomegalovirus immediate-early promoter (CMV promoter), followed by the first intron of human growth hormone, target cDNA, and a simian virus 40 polyadenylation signal sequence (SV40 poly(A)), between the inverted terminal repeats of the AAV-2 genome. The plasmids pAAV-LacZ, pEGFP, pAAV-AADC, pAAV-GCH, pCre, and pCreER^{T2} contained the cDNAs of LacZ, EGFP, human AADC, human GCH, Cre recombinase with a nuclear localization signal [26], and Cre recombinase fused to a mutated form of the ligand-binding domain of estrogen receptor α (CreER^{T2})[27], respectively. The plasmid pAAV-floxed TH contained human TH1 cDNA flanked by two loxP sequences between the CMV promoter and the SV40 poly(A). To generate pAAV-EGFP/Red, a DNA fragment containing d2EGFP (BD Biosciences, San Jose, CA, USA) and the SV40 poly(A) was flanked by loxP sequences and inserted between the CMV promoter and DsRed-Express-DR (BD Biosciences). The two helper plasmids, pHLP19 and pladeno1 (Avigen, Alameda, CA, USA), harbored the AAV *rep* and *cap* genes, as well as the *E2A*, *E4*, and *VA RNA* genes of the adenovirus genome, respectively. HEK293 cells were cotransfected by the calcium phosphate coprecipitation method with the vector plasmid, pHLP19, and pladeno1. The AAV vectors were then harvested and purified by two rounds of continuous iodoxale ultracentrifugations. Vector titers were determined by quantitative DNA dot-blot hybridization or by quantitative PCR of DNase I-treated vector stocks. We routinely obtained 10^{12} to 10^{13} vector genome copies (vg).

In vitro transduction. HEK293 cells were seeded at 3×10^5 cells/well in six-well plates. After 24 h, cells were infected with appropriate combinations of AAV vectors (5×10^9 vg per vector). 4-OHT was added to the culture medium at a concentration of 10 or 100 nM at 5 h after infection. Culture medium was collected for dopamine assay 48 h after infection and the cells were fixed for immunostaining.

AAV injections. All animal experiments were performed in accordance with the institutional guidelines. Three B6,129-*Gt(ROSA))26Sor*^{tm2Sho}/J mice (The Jackson Laboratory, Bar Harbor, ME, USA) [10] were stereotaxically injected into the caudoputaminal unit or cerebral cortex with 1×10^9 vg (1 μl) of AAV-CreER^{T2}. After 1 week, 4-OHT (1 mg) was administered intraperitoneally every day for 5 days, after which 2 of the mice were killed. One mouse that did not receive 4-OHT treatment was killed as a control. Creation of PD model rats and stereotaxic injections of AAV vectors were carried out as previously described [5]. Briefly, 60 male albino Wistar rats (weighing 200–250 g) were unilaterally lesioned at the left medial forebrain bundle (coordinates AP −4.3 mm and ML 1.6 mm, relative to the bregma, and DV −7.8 mm relative to the dura, with the incisor bar set 3.3 mm below the interaural line) with 4 μl of 4.5 mg/ml 6-OHDA HBr (Sigma, St. Louis, MO, USA) in 0.02% ascorbate saline prior to intrastriatal transduction. These rats were stereotaxically injected with AAV vectors (5×10^7 vg per site for each vector) at three sites in the lesioned striatum (coordinates relative to the bregma and dura, AP +1.5, +1.0, and +0.5 mm; ML 2.6, 3.0, and 3.2 mm; DV −5.2 mm). Forty-eight rats were injected with a 1:1:1 mixture of AAV-floxed TH, AAV-AADC, and AAV-GCH plus AAV-Cre (n = 12) or AAV-CreER^{T2} (n = 36). Twelve rats received AAV-LacZ alone as a control. Among the AAV-CreER^{T2}-treated rats, 24 were intraperitoneally injected with 4-OHT (4 mg/kg) for 5 consecutive days, starting either at the same time as or 4 weeks after vector injection.

Behavioral testing. The rats were tested weekly for rotational behavior and spontaneous limb use, as described previously [28]. The total number of complete body turns was counted during an observation period of ≥ 60 min following intraperitoneal injection of apomorphine HCl (0.1 mg/kg; Sigma). Only those animals exhibiting seven or more contralateral rotations/min in a 60-min period at 4 weeks after the 6-OHDA injection were included in further analysis. Spontaneous limb use was scored according to the cylinder test method [29]. Rats were placed in a clear glass cylinder large enough to ensure free movement. After they had performed 10 rears during which they were observed to place at least one paw on the cylinder wall, the number of times both forepaws contacted the wall of the cylinder was counted until at least 20 contacts were made. Data indicating the number of times a contralateral forepaw made contact with the wall are expressed as a percentage of the total. We also evaluated rotational behavior in response to a low dose of L-dopa methyl ester (5 mg/kg; Sigma) coadministered with 2.5 mg/kg of a peripheral decarboxylase inhibitor (benserazide hydrochloride; Sigma) 10 weeks after AAV injection.

Biochemical assays. Levels of dopamine in the cell culture medium (n = 4 for each group) and within the brain samples (n = 4 for each group) were determined by high-performance liquid chromatography (HPLC), as previously described [5]. Rats were killed by decapitation under sodium pentobarbital anesthesia 12 weeks after vector injection, after which their brains were immediately dissected and placed on dry ice. The striatum was punched out bilaterally using a sharp-edged, stainless steel tube. Wet tissue samples were weighed and stored at −80°C until subsequent analysis. Tissues were homogenized in 20 volumes of homogenization buffer and then mixed immediately with 0.76 M perchloric acid prior to centrifugation at 15,000*g* for 10 min. After the supernatant was neutralized with sodium acetate, the samples were analyzed by HPLC analysis. Determination of TH activity was based on the formation of L-dopa from L-tyrosine, as demonstrated by HPLC electrochemical detection. The reaction mixture contained 200 mM sodium acetate buffer (pH 6.0), 100 mM 2-mercaptoethanol, 0.2 mg/ml catalase, 0.2 mM L-tyrosine, and 1 mM tetrahydrobiopterin. The mixture was incubated for 10 min at 37°C. The reaction was stopped by adding perchloric acid, and L-dopa was extracted using an alumina column [30].

Immunostaining of cultured cells and brain sections. Cultured cells were fixed in 4% paraformaldehyde (PFA) in PBS. Brains were perfused with 4% PFA, soaked in 30% sucrose, and dissected into coronal sections (30 μm). The following primary antibodies were used: TH monoclonal (1:800 or 1:8000; DiaSorin, Stillwater, MN, USA) or polyclonal (1:10,000; provided by Ikuko Nagatsu, Fujita Health University, Japan), AADC polyclonal (1:10,000; I. Nagatsu), Cre recombinase monoclonal (1:500; Covance, Princeton, NJ, USA) or polyclonal (1:500; Covance), GFP polyclonal (1:200; BD Biosciences or Chemicon, Temecula, CA, USA), DsRed